THE EFFECT OF WALL FRICTION IN COMPRESSION-PERMEABILITY TESTING

by

Frank Leslie Rawling, Jr.

A Dissertation Submitted to the
Graduate Faculty in Partial Fulfillment of
The Requirements for the Degree of
DOCTOR OF PHILOSOPHY

Major Subject: Chemical Engineering

Approved:

Signature was redacted for privacy.

In Charge of Major Work

Signature was redacted for privacy.

Head of Major Department

Signature was redacted for privacy.

Dean of Graduate College

Iowa State University
Of Science and Technology
Ames, Iowa

1964

TABLE OF CONTENTS

NOMENCLATURE

A - septum area, ft^2

C - volume of filtrate attributed to the septum when the septum is considered as a fictitious weight of cake, ft^3

d - diameter, ft.

D - diameter of cell used in 4H/D, ft. or in.

g_c - proportionality constant relating force and mass, 32.2 $lb_m ft/lb_f sec^2$

h - height of a fluid column causing flow through a porous mass, ft. or cm.

H - cake thickness used in 4H/D, ft. or in.

J - Tiller's J factor

K - Ruth's parameter in the equation $(V + C)^2 = K(\theta + \theta_c)$

K_1 - parameter in equation 9

k - permeability constant in equations 1 and 2

k_o - permeability constant in equation 3

L - bed thickness or cake thickness, ft.

m, n - constants in equation 9

m - mass ratio of wet cake to dry cake

P - pressure, lb_f/ft^2

P_x - liquid-pressure at a distance x from the cake-septum interface, lb_f/ft^2

P_1 - liquid-pressure at cake-septum interface, lb_f/ft^2

P_{sx} - solids compressive-pressure at a distance x from the cake-septum interface, lb_f/ft^2

q - flow rate per unit of filter area or superficial velocity, $ft^3/ft^2 sec$

q_x - superficial velocity at a distance x from the cake-septum interface, ft^3/ft^2sec

q_1 - superficial velocity at the cake-septum interface, ft^3/ft^2sec

R_m - septum resistance, 1/ft.

S_1 - surface area of particles to total volume of porous mass, ft^2/ft^3

S_o - specific surface of solids, area of particles to volume of particles, ft^2/ft^3

s - ratio of the mass of solids to mass of slurry

V - filtrate volume, ft^3

W - mass of solids in filter cake, lb_m

α_{avg} - average specific resistance for compressible filter cakes, ft/lb_m

α_x - point specific resistance at a distance x from the cake-septum interface; specific resistance obtained from compression-permeability testing, ft/lb_m

ϵ - porosity, ratio of void volume to cake volume

ϵ_x - point porosity at a distance x from the cake-septum interface; porosity obtained from compression-permeability testing

θ - time, seconds

θ_c - time necessary to collect filtrate volume C, seconds

μ - viscosity, lb_m/ft_{sec}

ρ - liquid density, lb_m/ft^3

ρ_s - solids density, lb_m/ft^3

ABSTRACT

The phenomenon of wall friction between the filter cake and the test cell wall in a compression-permeability test cell has been investigated and its effect on the point specific filtration resistance has been determined.

An experiment was designed to measure the point specific resistance, α_x, as a function of filter cake weight at a constant applied pressure. The results of the experiment indicated that point specific resistance decreased as cake weight increased and that a cubic relationship in cake weight fit the data.

A second experiment was designed to test for wall friction. Two test cells differing only in diameter were operated under the same applied pressure and with cakes of the same thickness. Split-plot analysis of variance and polynomial regression techniques indicated a significant difference in the point specific resistance of the filter cakes in each cell. This difference between point specific resistances has been attributed to the effect of wall friction between the cake and the wall of the test cell chamber.

It has been shown that if point specific resistance is plotted against the ratio of wall area in contact with the cake to cross-sectional area, $4H/D$, where H is cake thickness and D is cell diameter, a straight line results. Furthermore

this plot removes the difference between the point specific resistances obtained at the same thickness and applied pressure in the two test cells. By extrapolating the straight line to zero 4H/D the point specific resistance of a differential element of filter cake is obtained.

INTRODUCTION

The fundamentals of fluid flow through porous media are applicable to many areas in the field of chemical engineering. One of these is filtration which is defined as the separation of solids from fluids by a filter medium which permits the flow of the fluid but retains the solids. There are other ways of separating solids from fluids, such as centrifugation or pressing. However, filtration is by far the most important industrially.

Although filtration is one of the most widely used unit operations it is one of the least understood, and industrial equipment for filtration has been developed largely by rule-of-thumb techniques rather than by application of theory. This is due in part to the inadequacy of theory to account for the complexity of the porous mass making up the filter cake and in part to the difficulty in obtaining reproducible results on laboratory equipment.

Since filtration is a special case of flow through porous media the variables affecting the latter must be investigated in order to gain a clear insight into the operation. These variables are flow rate, pressure drop, nature of the solids composing the media, porosity, and the degree of compressibility of the media. The porosity, which is the fractional ratio of void volume to total volume, of the medium is mainly a

function of the orientation of the particles, the frictional drag forces, and the applied pressure. The compressibility of the medium is difficult to measure accurately without knowing a great deal about the material itself and the structure of the porous mass.

Prior to the introduction of the compression-permeability cell concept, laboratory filtrations were carried out on small pilot plant filters. Correlation of results from such filtrations was generally not possible due to the variation of porosity, and thus resistance, throughout the filter cake. In an attempt to provide this correlation, Ruth (39) proposed the concept of specific resistance and devised the compression-permeability test cell as a means of conducting laboratory filtrations. In such a cell the mechanical pressure on the solids can be applied independently of fluid friction or drag. Resistance to fluid flow through the filter cake can then be measured directly using a liquid head which is small compared to the applied mechanical pressure. There are certain assumptions involved in interpreting test cell data. Tiller (53) enumerates these as follows:

1. Ultimate values of porosity are attained instantaneously.
2. There is point contact between particles.
3. The point filtration resistance of a given solid is determined by the porosity, which in turn depends

upon the solid compressive pressure P_{SX}.

4. The porosity or specific filtration resistance determined under a given mechanical loading, P_{SX}, in a compression-permeability cell is the same as the resistance at a point in the filter cake where the solid pressure (computed by $P_{SX} = P - P_X$) is the same as the mechanical loading in the compression-permeability cell.
5. Flow is viscous.

The first assumption is probably valid for filtrations in which pressure increases slowly. The second assumption leads to the basic equation $P_X + P_{SX} = P$, where P_X is the hydraulic pressure, P_{SX} is the solid compressive pressure, and P is the applied pressure.

In effect, values of porosity and specific resistance determined in the test cell are assumed to be the values which would exist in an infinitesimal layer of filter cake under the same mechanical pressure.

Though the advent of the compression-permeability cell spurred research in filtration, it is still difficult to correlate the data. The usual method of correlation has been to compare specific resistance values from test cell data with those obtained from constant pressure filtrations. In too many instances such comparisons fail to agree. In addition, recent work at Iowa State University (65) has cast some doubt

on the foregoing assumptions. Also, it is often difficult to obtain reproducible values of specific resistance from the test cell. It has been hypothesized that wall friction between the filter cake and the wall of the test cell may account for part of the spurious results obtained from test cell data.

The purpose of this thesis was to investigate the effect of wall friction in the compression-permeability test cell by determining its magnitude, if it exists, and then determining how it affects the specific resistance of the filter cake.

REVIEW OF THE LITERATURE

The literature on fluid flow through porous media and filtration is voluminous. Nevertheless, almost all of the work carried out in these fields for the past one hundred years uses as its base a publication by Darcy in the year 1856 (14). In the appendix to this publication Darcy proposed an equation relating the flow rate through a porous mass to the liquid head and the length of the bed. This equation, as given by Hubbert (27), is

$$q = -k(h_2 - h_1)/L \qquad (1)$$

or, in differential form

$$q = -k(dh/dL) \ . \qquad (2)$$

The proportionality factor k in equations 1 and 2 is a coefficient depending upon the permeability of the bed. By experimentation it can be shown that k is inversely proportional to the viscosity of the fluid. Thus a new factor, k_o, can be defined such that

$$q = \frac{-k_o}{\mu}(dh/dL) \ . \qquad (3)$$

In this form Darcy's equation becomes similar to the well-known Hagen-Poiseuille equation

$$q = \frac{g_c d^2}{32\mu}(dh/dL) \ . \qquad (4)$$

Equation 4 treats flow through long, straight tubes. The similarity between equations 3 and 4 has led many investiga-

tors over the years to treat flow through porous media as a special case of the Hagen-Poiseuille equation; thus treating the porous media as a bundle of capillary tubes. As Hubbert (27) points out, this is in error since, in reality, the Hagen-Poiseuille equation is a very special case of Darcy's equation.

Following the development of these equations, it is apparent that in comparing equations 3 and 4 k_o was thought to be proportional to the square of the diameter of an equivalent channel. Seelheim (45) proposed a term which used the effective particle size as the diameter of the channel. However, Seelheim's equation did not take into consideration changes in porosity. Dupuit (16) made the assumption that the fractional free area of sand bed cross-sections was constant for a given bed and equal to the porosity. The flow rate thus became q/ϵ. Eventually, workers in the field came to regard particle size as a measure of specific surface, S_o, rather than as an equivalent particle diameter, since a fluid flowing in the laminar region encounters resistance dependent upon the exposed surface. For spherical particles $S_o = 6/d$ and for non-uniform particles an effective diameter $d_m = 6/S_o$ can be defined. Kruger (33) was the first to make use of this principle, using it in his studies of sands with porosities ranging from 0.30 to 0.40.

In 1927 Kozeny (32) published his classic paper on the

theory of ground-water movement. In this paper Kozeny treated the porous medium as a collection of channels of various cross-sections but of different length. He proceeded to solve the Navier-Stokes equations simultaneously for all channels passing through a cross-section normal to the flow in the porous medium. He then expressed the permeability in terms of the specific surface, S_1, of the porous medium. The following equation resulted:

$$q = - \frac{C\epsilon^3}{(\mu S_1^2)} \Delta P \ , \qquad (5)$$

where C is a pure number depending only upon the form of the cross-section; for circular cross-sections C has a value of 0.50. In comparison with equation 2 the permeability, k, in Darcy's equation is

$$k = \frac{C\epsilon^3}{S_1^2} \qquad (6)$$

in equation 5. In 1937 Carman (9) modified k in the following manner

$$k = \frac{\epsilon^3}{k_1 S_o^2 (1-\epsilon)^2} \qquad (7)$$

and obtained the so-called Kozeny-Carman equation

$$q = \frac{\epsilon^3 g_c}{(1-\epsilon)^2 k_1 \mu S_o^2} \cdot \frac{\Delta P}{L} \qquad (8)$$

where k_1 is usually taken as 5.0. It should be noted that S_1 and S_o in the preceding equations are not the same. S_1 in

Kozeny's equation is the specific surface of the porous medium, whereas S_o in Carman's equation is the specific surface of the solid. Also, in equations 7 and 8, $C = \frac{1}{k_1}$ and Carman's value of 1/5 for this is at variance with Kozeny's value of 1/2. A few years later the Kozeny equation was developed independently in America by Fair and Hatch (17).

Early workers in the field of filtration developed equations from laboratory experimentation rather than from theory as did Kozeny. Many of these workers failed to recognize that Darcy's Law could be applied to filtration. Almy and Lewis (1) using a laboratory plate and frame filter press developed empirically the equation

$$R = k_1 \frac{P^m}{v^n} \qquad (9)$$

to describe the rate of flow of filtrate as a function of filtrate volume and pressure. Like Baker (4), and Webber and Hershey (63), they employed equipment with which it was almost impossible to obtain reproducible results. Sperry (47, 48, 49) was one of the first workers who attempted to improve the collection of data and thus obtain more accurate results. He devised a method to continuously record the time-discharge rate of filtrate. Essentially this was a float to which was attached a pen holder. The pen inked a curve on a cylinder driven at one revolution per hour by a clock. Sperry (50) criticized the equation proposed by Baker (4) on the grounds

that no provision was made for distinguishing between the resistance due to the filter cloth and that due to the filter cake. As far back as 1908 Hatscheck (24) had noticed that the resistance of cloth with a thin layer of cake was much greater than the sum of the resistance of the cake plus the resistance of the cloth. Thus he emphasized the importance of the first layer of filter cake to be laid down.

In 1926 Hinchley and Ure (26) stated that if the analogy of flow through capillary tubes is used to explain filtration phenomena then the rate of flow should follow Poiseuille's Law. Van Gilse et al. (57, 58, 59, 60) determined that the rate of flow was independent of the volume from which the cake was formed and depended only upon the quantity of solids in the filter. That is, the initial concentration of the slurry did not determine the rate of flow. In addition, Van Gilse and his coworkers determined that when the resistance of the filter cloth was close to zero, graphs of volume of filtrate vs. time are parabolas. They also stated that all layers of the filter cake are subjected to the same pressure drop, are equally compressed, and thus have the same resistance. Later work by Ruth (41, 42, 43) indicated this to be in error. Van Gilse and his colleagues also showed that the resistance of filter cakes in constant pressure filtrations could be expressed as a linear function of the pressure. This was a marked advance over the Lewis equation (62) where r varied

as P^{s-1}.

In 1931 the first of a series of papers by Ruth and associates at the University of Minnesota appeared (41). The result of these papers was to bring about a major change in theoretical and experimental work in filtration. From experimental data Ruth was able to deduce the following equation

$$(V+C)^2 = K(\theta+\theta_c) \quad . \tag{10}$$

This equation is a form of the theoretical law

$$V^2 = K\theta \tag{11}$$

which holds for the entire course of a particular constant pressure filtration. Ruth considered the constant C as "the resistance of a layer of solids which would be separated from C liters of filtrate in an imaginary filtration beginning with zero resistance to filtrate flow." Ruth claimed that a single general equation held for all classes of material whether compressible or incompressible. He thereupon formulated the following fundamental axiom of constant pressure filtration (43):

> The time-volume curve of a properly performed constant pressure filtration forms a portion of a perfect parabola, of which the missing part near the vertex represents the theoretical course of a similar filtration which would generate a resistance to filtrate flow equal to that already existing when measured filtrate volume is zero.

In Ruth's treatment the constant in equation 10 is obtained from the differential form of the equation

$$\frac{d\theta}{dV} = \frac{2V}{K} + \frac{2}{K} C \tag{12}$$

Plotting dθ/dV vs. V results in a straight line with slope 2/K. The average specific resistance of the filter cake material is related to the slope 2/K by the following equation:

$$\alpha_{avg} = \frac{2A^2 \Delta P(1-ms)g_c}{K\mu\rho s} . \qquad (13)$$

The filtration equation, employing cake weight, written in differential form is

$$\frac{1}{A}\frac{dV}{d\theta} = \frac{g_c \Delta P}{(\frac{W\alpha_{avg}}{A} + R_m)\mu} , \qquad (14)$$

R_m being the septum resistance. Equation 14 has been employed by a number of investigators (3, 6, 11, 12, 18, 19, 31, 40, 47).

Since equation 14 is a form of Darcy's equation it can be compared to the Kozeny-Carman equation. If the Kozeny-Carman equation is written in terms of cake weight,

$$q = \frac{\epsilon^3}{(1-\epsilon)} \cdot \frac{\rho_s g_c \Delta P}{k_1 \mu S_o^2 \frac{W}{A}} \qquad (15)$$

results. If the resistance of the septum is neglected then

$$\alpha_{avg} = \frac{k_1(1-\epsilon)S_o^2}{\epsilon^3 \rho_s} . \qquad (16)$$

Ruth's inception of the compression-permeability cell in 1946 (39) has spurred a large amount of research in filtration. Among those using the cell, Grace's work in the early 1950's is of importance (19, 20, 21).

Grace applied the Kozeny-Carman equation to the filtra-

tion of compressible cakes. He determined that the compressible nature of most filter cakes is due to particle flocculation in the feed suspension. Specifically, the greater the degree of flocculation the lower the specific resistance of the filter cake. However, due to the greater flocculation, the cake is more compressible. Grace also found that the Kozeny-Carman equation cannot be employed in the usual manner when applied to compressible filter cakes. Because of the flocculation phenomena the specific surface of the particles, S_o, must be calculated from the particular feed suspension being used while at the same time the compressive pressure during filtration must be taken into account. Should independent values of S_o and particle size be obtained, highly inaccurate values of specific resistance result. Grace's experimental results indicated that if thickness-to-diameter ratio for the compression-permeability cell did not exceed 0.6, the effect of wall support and bridging was negligible and the porosity and pressure distribution within the compression-permeability cell were uniform.

During the last decade the compression-permeability cell has been used by other investigators (19, 25, 28, 29, 31, 34, 36, 61, 64, 65).

In 1953, Tiller published the first of a series of papers on the role of porosity in filtration (51, 52, 53). For the first time the assumptions underlying the use of the com-

pression-permeability cell were explicitly stated (53). The average specific resistance as first defined by Ruth (39) was given as

$$\alpha_{avg} = \frac{P}{\int_0^P \frac{dP_{sx}}{\alpha_x}} . \qquad (17)$$

Equation 17 is derived on the assumption that α_{avg} is a function only of solids pressure, P_{sx}. Tiller's work has centered around modifying and improving this equation. In a constant pressure filtration the rate of filtration decreases as the cake builds up. For such a case Tiller (51) rewrote equation 15 as follows:

$$\frac{s\rho\mu}{1 - ms} \frac{K}{g_c} \frac{S_o^2}{\rho_s} \frac{V}{A^2} \frac{dV}{d\theta} = \frac{V}{CA^2} \frac{dV}{d\theta} = \int_{P_1}^{P} \frac{\epsilon^3}{1 - \epsilon} dP_x . \qquad (18)$$

For constant ϵ

$$\frac{s\rho\mu}{1 - ms} \frac{K}{g_c} \frac{S_o^2}{\rho_s} \frac{V}{A^2} \frac{dV}{d\theta} = \frac{\epsilon^3}{1 - \epsilon} \int_{P_1}^{P} dP_x = (P - P_1) \frac{\epsilon^3}{1 - \epsilon} \qquad (19)$$

$$\frac{kS_o^2(1-\epsilon)}{\rho_s \epsilon^3} \frac{s\rho\mu}{1 - ms} \frac{V}{A^2} \frac{dV}{d\theta} = P - P_1 \qquad (20)$$

or

$$\frac{\alpha_{avg}\, s\rho\mu}{1 - ms} \frac{V}{A^2} \frac{dV}{d\theta} = P - P_1 . \qquad (21)$$

For constant septum resistance

$$g_c P_l = \mu \frac{R_m}{A} \frac{dV}{d\theta} , \tag{22}$$

therefore

$$\frac{d\theta}{dV} = \frac{\alpha_{avg}}{P} \frac{s\rho\mu V}{(1-ms)A^2} + \frac{\mu R_m}{g_c AP} . \tag{23}$$

For zero filtrate volume

$$P_l = P = \frac{\mu R_m}{g_c A} (dV/d\theta)_\theta = 0 . \tag{24}$$

Thus when septum resistance is known initial filtration rates can be calculated. Tiller also redefined α_{avg} as

$$\alpha_{avg} = \frac{P - P_l}{\int_{P_l}^{P} \frac{dP_{sx}}{\alpha_x}} . \tag{25}$$

Substituting in P_l from equation 22

$$\alpha_{avg} = \frac{P - \frac{\mu R_m}{g_c A} \frac{dV}{d\theta}}{\int_0^P \frac{P - \frac{\mu R_m}{g_c A} \frac{dV}{d\theta}}{\alpha_x} dP_{sx}} . \tag{26}$$

Using these equations, Tiller showed that plots of $d\theta/dV$ vs. V are virtually straight but deviate from linearity at the beginning of the filtration.

Tiller showed (53) that α_x values can be determined indirectly from α_{avg} values obtained from equation 14. This equation can be rewritten as

$$q = \frac{\Delta P\, g_c}{(w\alpha_{avg}+R_m)\mu}\,, \tag{27}$$

where $w = W/A$ and $q = dV/(Ad\theta)$, and

$$\alpha_{avg} = \frac{\frac{g_o \Delta P}{q\mu} - R_m}{w}\,. \tag{28}$$

If $g_c \Delta P/(q\mu)$ is plotted against w then α_{avg} is the tangent of the angle $(g_c \Delta P/(q\mu),\ R_m,\ g_c \Delta P/(q\mu)-R_m)$. By use of equation 28 α_{avg} vs. $P - P_1 = P_s$ can be obtained. Then since

$$\alpha_{avg} = \frac{P - P_1}{\int_0^{P - P_1} \frac{dP_{sx}}{\alpha_x}} = \frac{P_{sx}}{\int_0^{P_{sx}} \frac{dP_{sx}}{\alpha_x}} \tag{29}$$

$$\frac{P_{sx}}{\alpha_{avg}} = \int_0^{P_{sx}} \frac{dP_{sx}}{\alpha_x}\,. \tag{30}$$

Differentiating equation 30 with respect to P_{sx} gives the following:

$$\frac{dP_{sx}}{\alpha_x} = \frac{\alpha_{avg}\, dP_{sx} - P_{sx} d\alpha_{avg}}{\alpha_{avg}^2} \tag{31}$$

or

$$\alpha_x = \frac{\alpha_{avg}}{1 - \frac{d\ln\alpha_{avg}}{d\ln P_{sx}}}\,. \tag{32}$$

Tiller and Cooper (54) took into consideration the fact that both m and ϵ_x change in a filter cake from the surface of

the cake to the medium. If the average porosity decreases then q_x will vary through the cake, reaching its maximum value at the cake-septum interface. By a liquid material balance over a differential section of the cake, the equation

$$\frac{\partial q_x}{\partial x} = - \frac{d\epsilon_x}{dP_{sx}} \frac{\partial P_{sx}}{\partial \theta} \tag{33}$$

results, x being measured from the cake surface. The basic equation describing flow through a porous compressible solid is

$$- g_c \frac{dP_x}{dx} = g_c \frac{dP_{sx}}{dx} = \alpha_x \mu \rho_s (1-\epsilon_x) q_x \ . \tag{34}$$

Equations 33 and 34 are simultaneous equations with P_{sx} and q_x as dependent variables. These equations can be combined to eliminate q_x giving

$$g_c \frac{\partial^2 P_{sx}}{\partial x^2} = g_c \left(\frac{\partial P_{sx}}{\partial x}\right)^2 \frac{d}{dP_{sx}} \left[\ln \alpha_x (1-\epsilon_x)\right] -$$

$$\mu \rho_s (1-\epsilon_x) \left(\frac{d\epsilon_x}{dP_{sx}}\right) \left(\frac{\partial P_{sx}}{\partial \theta}\right) \ . \tag{35}$$

These equations are based on the assumption that α_x and ϵ_x are functions of P_{sx} only and that $-dP_x = dP_{sx}$.

Tiller and Cooper (55) also determined that a plot of ϵ_x vs. x takes on a variety of shapes for different materials subject only to the condition that ϵ_x decreases as the fluid flows from the surface of the cake to the medium.

Tiller and Shirato (56) noticed that when the average

specific resistance, α_{avg}, is a function of a variable flow rate through the cake, $\alpha_{avg} = f(P, s, dV/d\theta)$, where s is the slurry concentration. They define α_{avg} as

$$\alpha'_{avg} = \frac{J(P - P_1)}{\int_0^{P - P_1} \frac{dP_{sx}}{\alpha_x}} \tag{36}$$

where J is defined as

$$J = \frac{1}{q_1 w} \int_0^w q_x dw_x = \int_0^1 \left(\frac{q_x}{q_1}\right) d\left(\frac{w_x}{w}\right) . \tag{37}$$

Now it is seen that

$$\alpha'_{avg} = J\alpha_{avg} \tag{38}$$

and since $J = q_{avg}/q_1$, where q_{avg} is based upon integration with respect to w_x, J will be less than unity since q_{avg} is less than q_1, the flow rate at the septum.

Okamura and Shirato (36) examined the liquid pressure distribution in filter cakes during constant pressure filtrations. They found that liquid pressure distribution is independent of the volume of filtrate, V, concentration of slurry, s, and filtration pressure, P. The liquid pressure can be approximately described by the following equation

$$\frac{x}{L} = \frac{(P-P_x)^{\upsilon}}{P} , \tag{39}$$

where υ is unity for incompressible cakes and decreases with

increasing compressibility. These authors later determined (35) that agreement between liquid pressure distributions by direct measurement and the liquid pressure distributions estimated from compression-permeability experiments is not good. To estimate liquid pressure distributions Shirato and Okamura made use of a compression-permeability cell. However, their technique in using the cell differed from that normally employed. For a permeation experiment they would introduce distilled water into the hollow piston and apply pressure to it by compressed air. The piston, to which weights had been applied, would be fixed at a specific position. Normally the piston is free to move and a small liquid head compared to the mechanical loading of the cell is used. The data obtained by Shirato and Okamura were graphically integrated to obtain P_x at some x/L value using

$$\frac{x}{L} = \frac{\int_{P_x}^{P} \frac{\epsilon^3}{k \cdot S_o^2(1-\epsilon)^2}\, dP_x}{\int_{0}^{P} \frac{\epsilon^3}{k \cdot S_o^2(1-\epsilon)^2}\, dP_x} . \qquad (40)$$

From further experiments (37, 46) Shirato and Okamura stated that there is always an equilibrium between cake compressive pressure and the porosity at a certain position in both isobaric and constant rate filtrations. Indeed they show that in comparing m from compression-permeability estimates

with isobaric filtrations a deviation of $\pm$ 4% is observed. A similar comparison shows that α_{avg} deviated by $\pm$ 2% and ϵ_{avg} and K (Ruth's parameter) deviated by only $\pm$ 3%. They also indicate that constant rate filtrations with pressures predicted from compression-permeability data show a deviation of 3% from constant rate.

In studying the behavior of Gairome-clay slurries Shirato and Okamura discovered that the specific resistance decreases with increasing cake thickness. The same phenomenon was observed by Willis (64) with calcium carbonate cakes.

The latest work performed with the compression-permeability test cell is that of Willis (65). He experimentally tested certain of the assumptions of Tiller (53). Willis found that the porosity at any instant in a filter cake confined in a test cell is not the equilibrium porosity. Further, he determined that the relationship $dP_{sx} = - dP_x$ as proposed by Tiller (53) does not hold but, rather, should be of the form $dP_{sx} = - \epsilon\, dP_x$. Willis further determined that though P_{sx} does determine ϵ_x, α_x is not solely determined by ϵ_x and P_{sx}. Thus α_x is affected by other factors.

In recent years there have been several papers dealing with aspects of filtration other than that of compression-permeability testing. Brenner (7) studied the unconfined growth of a filter cake on a circular filter cloth. This was an example of a three-dimensional filtration. Brenner was

able to solve analytically Laplace's equation for the instantaneous pressure distribution within the cake as well as the flow rate of filtrate through the filter cloth.

Burak and Storrow (8) studied the flow relationships in a basket centrifuge - sometimes called a hydroextractor. They treated the centrifuge as a filter placing four thicknesses of filter cloth on the inside of the basket and running the centrifuge over a range of 420 to 3000 rpm. Haruni and Storrow (22) studied cake formation in a hydroextractor and determined that cake formation may be altered by changing the method of feeding slurry to the basket. Haruni et al. (23) investigated flow through incompressible cakes in a hydroextractor. Bakker et al. (5) studied the influence of initial filtration velocity and of vibrations on the resistance of a polystyrene filter cake. They found that the influence of initial filtration velocity could be expressed mathematically but that the parameters in the equation also depended upon particle size.

A thorough review of the literature in porous media up to 1959 is given in an excellent monograph by Scheidegger (44).

EQUIPMENT AND PROCEDURE

Description of the Compression-Permeability Test Cells

Three test cells were used in this investigation. One of these cells, constructed of chrome-plated mild steel, was that used by Willis (64). This cell has a filter area of 2.074 square inches. The other two cells differed mainly in diameter and were constructed specifically for this study. The construction details of these two cells follow.

Small cell

The smaller cell, Figures 1 and 2, was constructed entirely of plexiglass with the exception of the porous stainless steel plates. The drainage base of the cell was machined from a 4-inch diameter cylinder of plexiglass. The hollow shaft was machined from a 2 1/2-inch diameter cylinder of plexiglass. The shaft has an inside diameter of 1.5180 inches. The piston was made from a 1.5000-inch outside diameter plexiglass tube with a 1/4-inch wall thickness. The top of the piston, which serves as a base plate for the applied weights, was made from a 4-inch diameter by 1 1/4-inch thick plexiglass blank. The porous stainless steel plates, one to form the septum and the other to form the bottom plate of the piston, were obtained from the Micro Metallic Division of the Pall Corporation. The plates are 3/16-inch thick and have a

Figure 1. Photograph of component parts of small test cell; diameter of chamber = 1.5180 inches

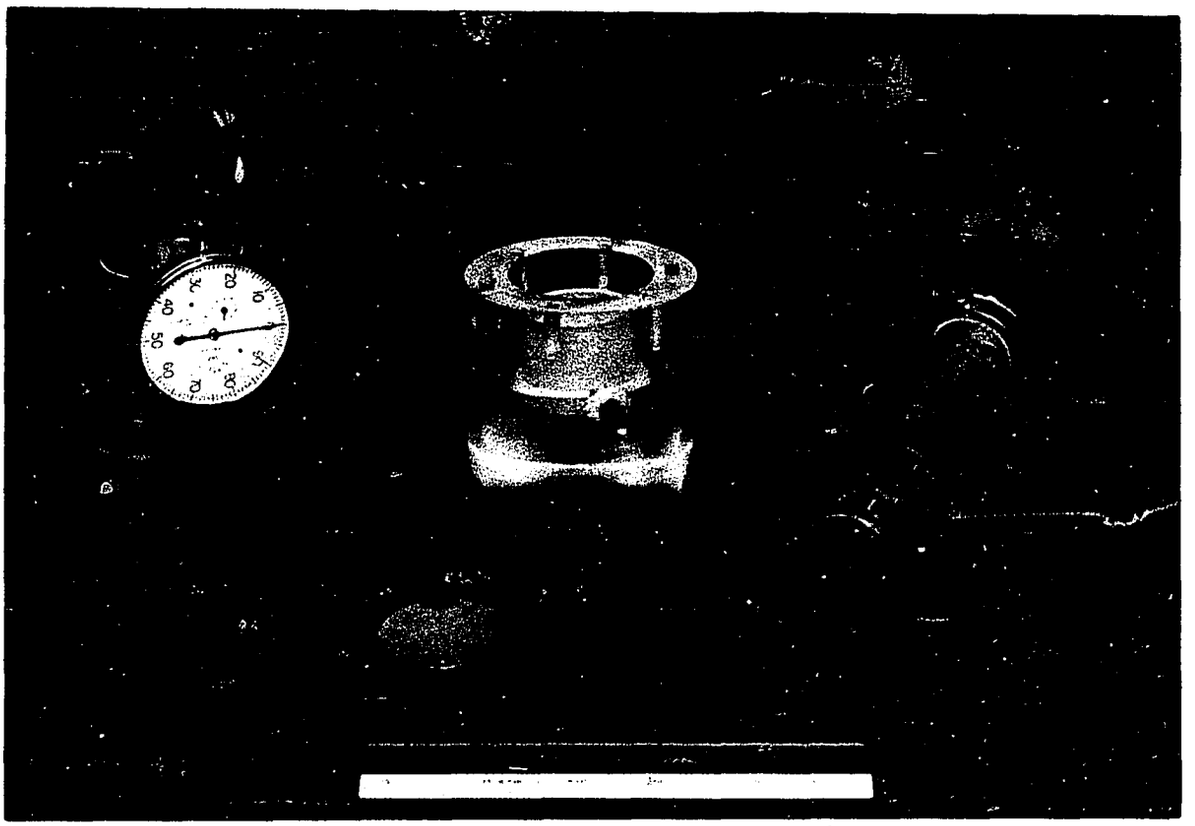

Figure 2. Detailed drawing of small test cell; diameter of chamber = 1.5180 inches

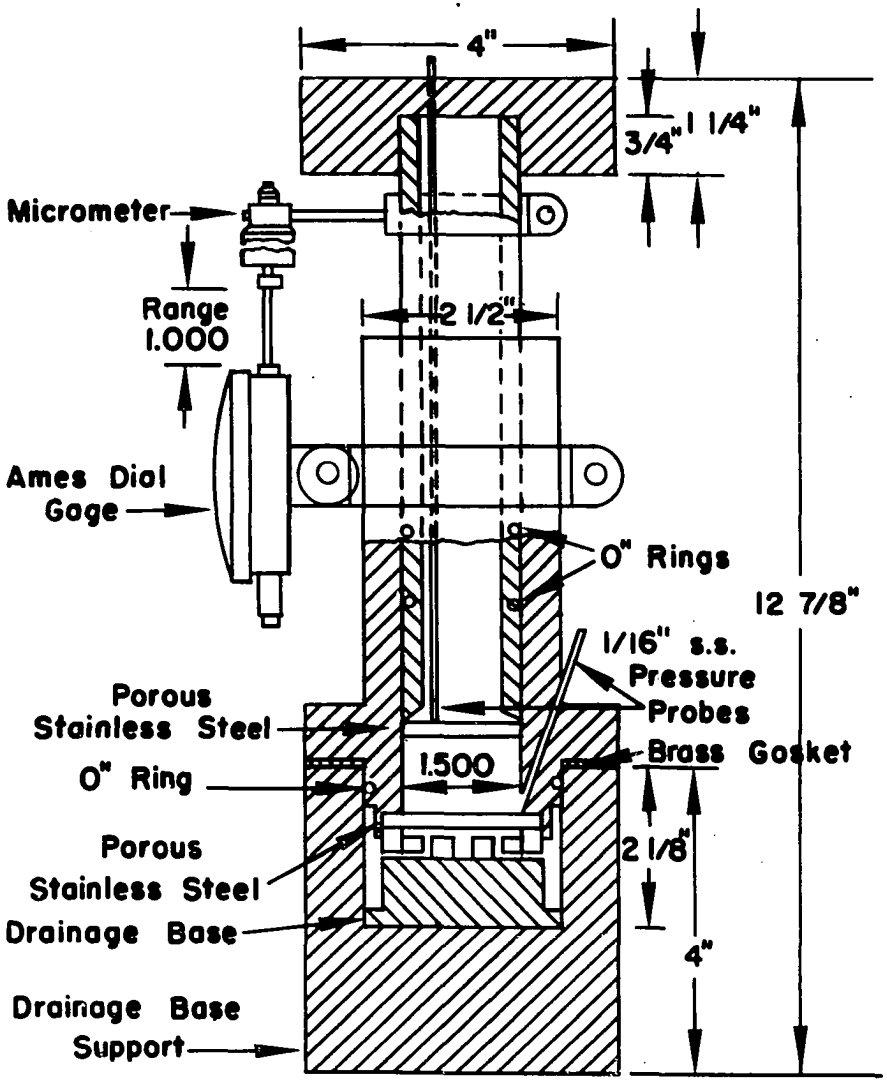
4"
3/4"
1 1/4"
Micrometer
Range
1.000
2 1/2"
Ames Dial
Gage
0" Rings
12 7/8"
1/16" s.s.
Pressure
Probes
Porous
Stainless Steel
Brass Gasket
0" Ring
1.500
2 1/8"
Porous
Stainless Steel
Drainage Base
4"
Drainage Base
Support

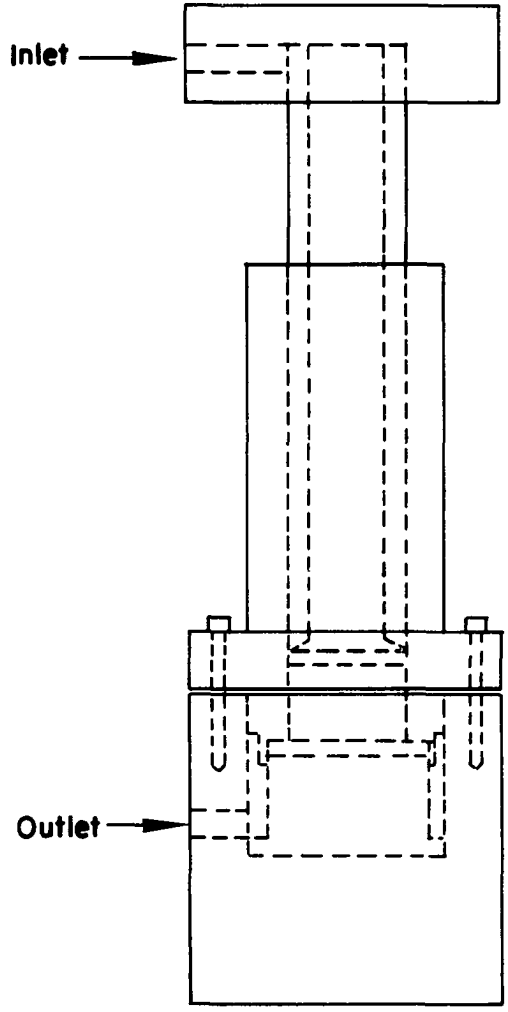
Inlet
Outlet

mean pore opening of 165 microns. The piston has two O-rings 1 inch apart to prevent filtrate leakage and piston wobble. The porous plate on the bottom of the piston was grooved around the edge to accommodate a brass ring used to secure the filter paper to the plate. A 1/16-inch inside diameter stainless steel tube was inserted through the length of the piston and terminated flush with the bottom face of the piston porous plate. This tube acts as a pressure probe. A second probe was inserted in the shaft wall and terminated in the septum chamber flush with the upper surface of the porous plate used as a septum. A 300-mesh copper screen was placed over the opening of this probe to prevent cake material from entering the probe. This cell has a filtering area of 1.8098 square inches.

Large cell

The large cell, Figures 3 and 4, is similar in design and construction to the small cell. It differs only in size. The drainage base was machined from a 7-inch diameter plexiglass cylinder. The hollow shaft was machined from a 5-inch diameter plexiglass cylinder. This hollow shaft has an inside diameter of 3.0100 inches. The piston was made from a plexiglass tube 3.0000 inches in diameter with a 1/4-inch wall thickness. The top of the piston, serving as a base plate for the applied weights, was made from a 7-inch diameter plexi-

Figure 3. Photograph of component parts of large test cell; chamber diameter = 3.010 inches

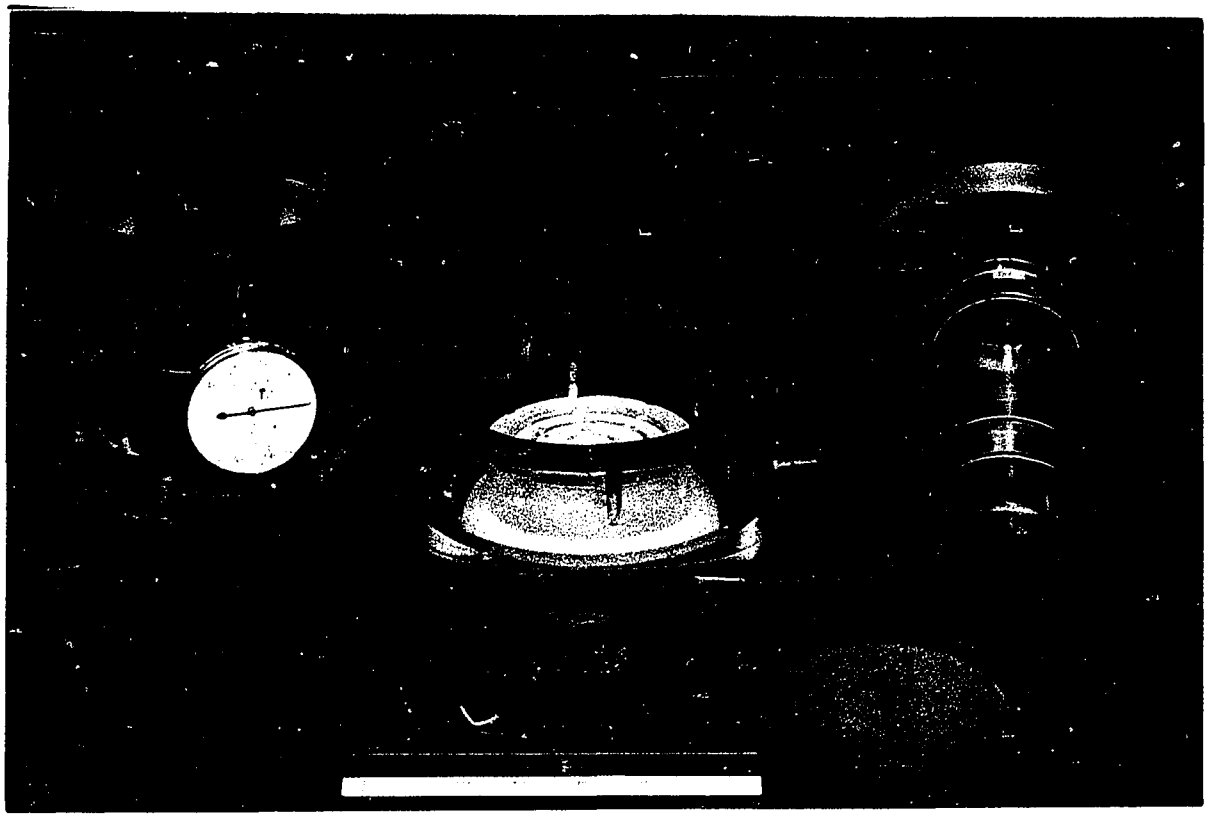

Figure 4. Detailed drawing of large test cell; chamber diameter = 3.010 inches

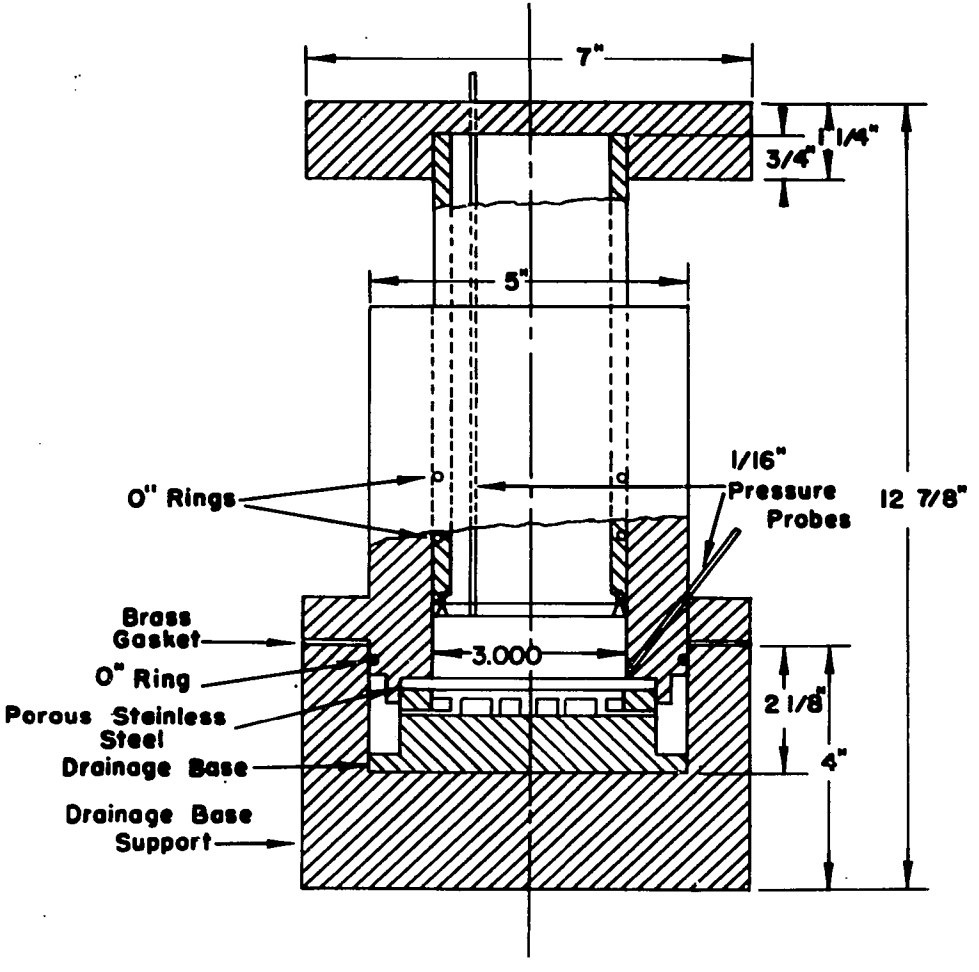
7"
1 1/4"
3/4"
5"
O" Rings
1/16"
Pressure
Probes
12 7/8"
Brass
Gasket
O" Ring
Porous Steinless
Steel
Drainage Base
Drainage Base
Support
3.000
2 1/8"
4"

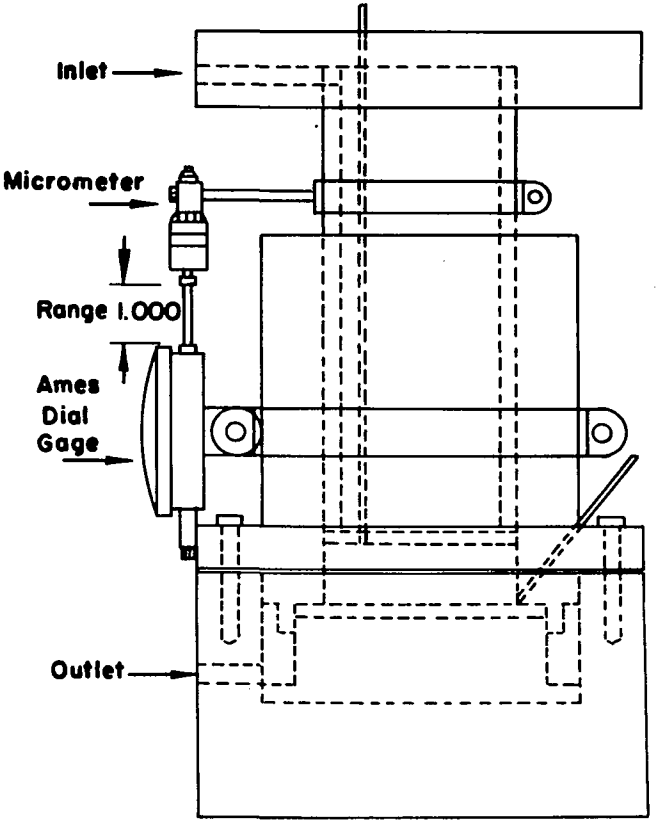
Inlet
Micrometer
Range 1.000
Ames
Dial
Gage
Outlet

glass blank.

Both cells were fitted with an Ames Dial Gage having a reversed dial. A micrometer, attached to the piston, actuates the gage in such a manner that the gage always reads the height of the piston above the septum. The maximum height that can be read from the dial gage is 1.0000 inches.

The compression-permeability cell system

The entire system for the compression-permeability test cells, Figures 5 and 6, consists of a constant head device made from an 8-liter aspirator bottle for the fluid feed, two manometers connected to the pressure probes, a self-levelling burette, 5- and 20-ml. burettes for flow rate measurements, a 4000-ml. graduated cylinder for filtrate collection, the test cell, and a clock and stopwatch.

Operating procedure

The operating procedure for the cells was to place a slurry of the material to be tested into the cell chamber, insert the piston, apply weights to the piston, pass clear filtrate through the cake, and measure the flow rate in the 5-ml. burette for the small cell and in the 20-ml. burette for the large cell.

When assembling the cells it was necessary to be sure that there was no air in the system. This was done by immers-

Figure 5. Photograph of test cell system

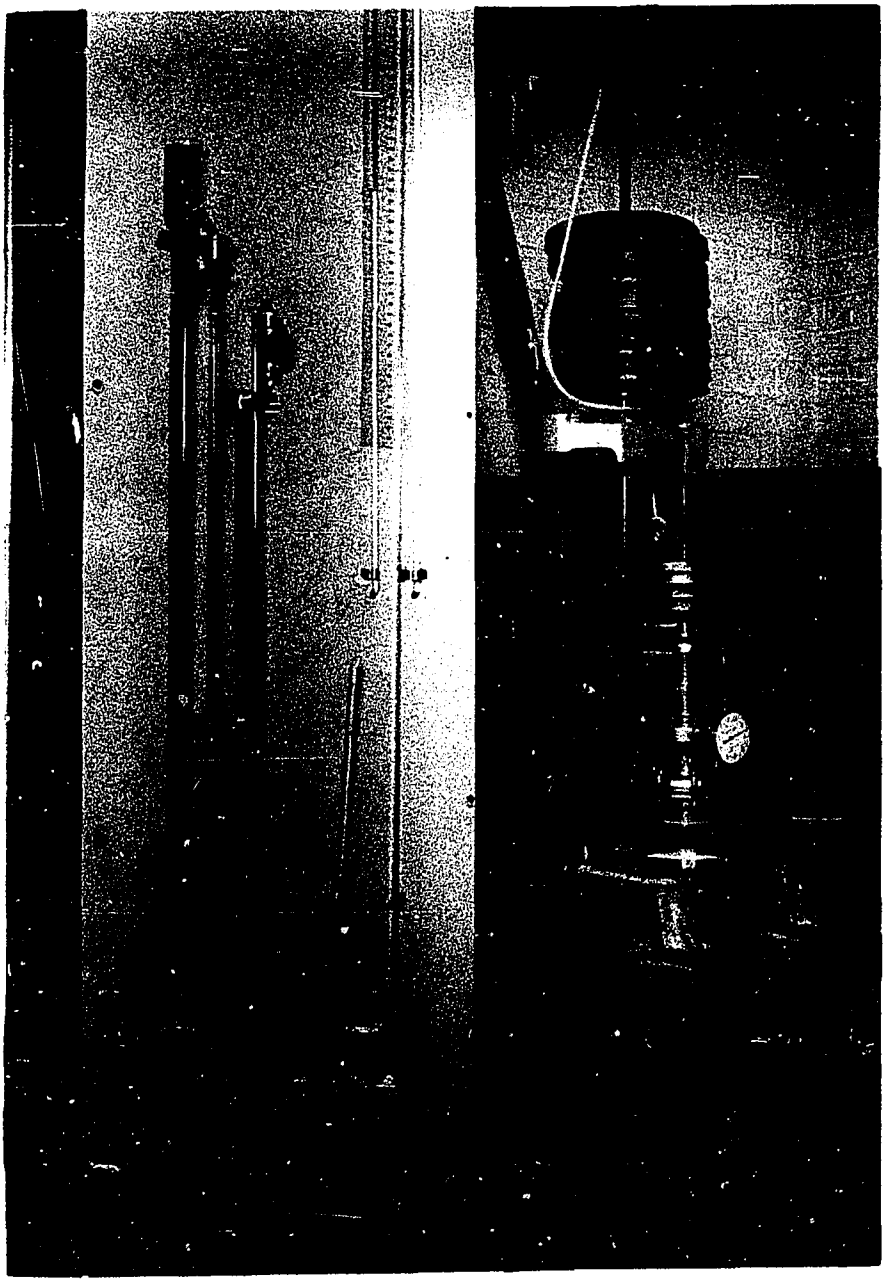

Figure 6. Drawing of test cell system

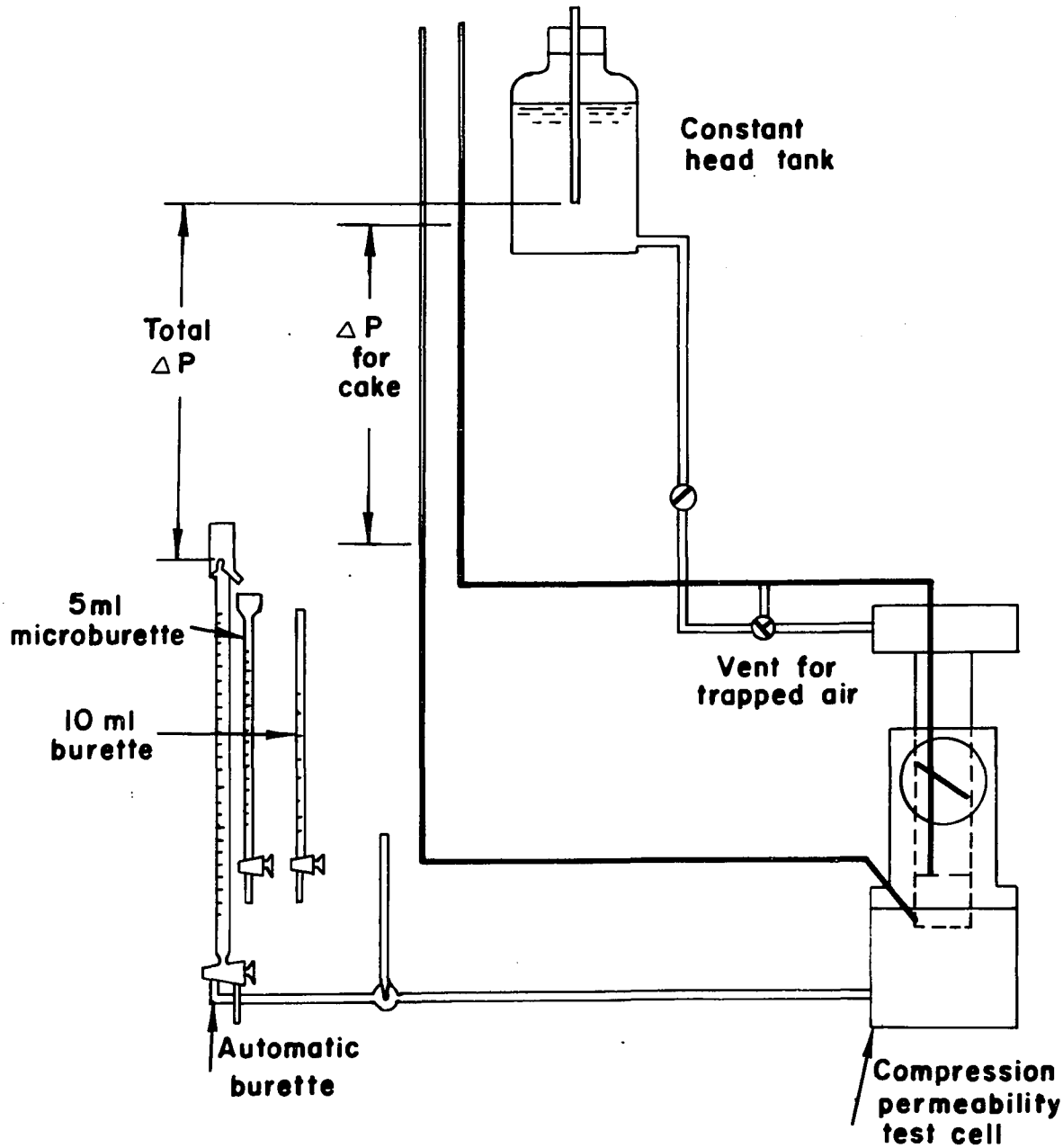
Constant
head tank
Total
ΔP
ΔP
for
cake
5ml
microburette
10 ml
burette
Vent for
trapped air
Automatic
burette
Compression
permeability
test cell

ing the drainage base and shaft in water, fitting the porous plate covered with filter paper into the shaft and then assembling them all under water. The tygon tubing on the outlet line was also connected to the outlet port while the cell was still immersed. Since the outlet tubing had been maintained full of water this insured that no air would be trapped in the system. The cell was removed from the water, excess water removed from the shaft and the slurry poured into the cylinder.

The piston was connected to the fluid feed system and filled with water. A piece of filter paper was placed over the porous plate and held on by the brass ring. The piston was then placed in the cylinder and the three-way stopcock in the feed line properly positioned. As the piston descended air was forced out through the piston and escaped to the atmosphere via the stopcock. When the piston stopped moving the required weights were applied to the top of the piston and the three-way stopcock positioned to allow fluid to flow from the constant head tank. The outlet valve was opened, manometer leads connected, and the run was started. The following readings were taken every 5 minutes for 1 hour: 1) manometers, 2) dial gage, 3) filtrate temperature, 4) flow rate, 5) accumulated filtrate.

In this investigation only reagent grade calcium carbonate was used.

RESULTS AND DISCUSSION

Part I. The Effect of Cake Weight on Specific Resistance

Shirato and Okamura (46), as well as Willis (64), reported experimental evidence indicating that point specific resistance decreases as cake thickness increases. Willis fit an hyperbola to his data. None of these investigators gave any explanation for this behavior, however.

To verify the existence of this phenomenon, an experiment was designed to measure the point specific resistance, α_x, as a function of cake weight. Cake weight was chosen because cake thickness is a function of other factors while cake weight can be fixed. If the same applied pressure is used the thickness of the cake varies with cake weight.

Because previous investigators (19, 52) reported that slurry concentration had an effect on point specific resistance, this variable was also included in the design. Thus the experiment was designed to test for the following factors: 1) effect of cake weight on point specific resistance, 2) effect of slurry concentration on point specific resistance. It was decided to test four cake weights and four slurry concentrations.

Since two factors were to be tested, each at four levels, a statistical design seemed appropriate. The experiment can be classified as a 4 x 4 or 4^2 factorial. The statistical

design that was chosen to incorporate the 4 x 4 factorial was a completely randomized block design. Such a design is applicable when observations are classified according to two different criteria (38).

In the design the two factors were the four concentrations and the four cake weights. The mathematical model for this design is

$$Y_{ij} = \mu + \beta_i + \tau_j + \epsilon_{ij} \; ; \qquad (41)$$

$$i = 1, \ldots, b$$

$$j = 1, \ldots, t,$$

and μ, β_i, and τ_j are constants such that

$$\sum_{i=1}^{b} \beta_i = \sum_{j=1}^{t} \tau_j = 0 \; . \qquad (42)$$

β_i represents the true effect of the ith level of concentration and τ_j represents the true effect of the jth level of cake weight, both being measured as deviations from the mean. The ϵ_{ij} are normally and independently distributed with mean 0 and variance σ^2, (NID $(0, \sigma^2)$). The performance of experiments of this type are influenced by the operator who carries out the work. This is usually called a time effect. To remove this effect the 16 runs were divided in half in such a fashion that each cake weight and each concentration appeared twice in each half. These two halves were coded early (E) and late (L) depending upon the order in which they were run. In addition, the sequence of run in each half was randomized.

The experiment is described in Table 1. The Roman numeral in each cell refers to the unit in the particular portion of the experiment, the Arabic numeral stands for the order of run in the portion and the letter refers to the particular half of the experiment, i.e. E stands for the early half. The experiment was run at an applied pressure of 27.023 psig and the length of each run was 20 minutes.

Table 1. Randomized block design of an experiment to test the effect of cake weight and slurry concentration on point specific resistance

Cake weight	Concentration			
	0.200 gms/ml	0.233 gms/ml	0.266 gms/ml	0.300 gms/ml
10.00 gms	I-5-E	I'-2-L	II-3-E	II'-8-L
16.66 gms	III'-5-L	III-6-E	IV'-1-L	IV-2-E
23.32 gms	V'-3-L	V-7-E	VI'-7-L	VI-4-E
30.00 gms	VII-1-E	VII'-6-L	VIII-8-E	VIII'-4-L

For each cell in the design a value of the point specific resistance was calculated. The values which appear in Table 2 were calculated for 1200 seconds. It was found that the porosity was relatively constant beyond this point in the run and thus the run was terminated.

Conclusions from the data were drawn statistically. The

Table 2. Values of point specific resistance, α_x, and cake thickness, L,[a] at 1200 seconds; applied pressure = 27.023 psig

Cake weight	Concentration			
	0.200 gms/ml	0.233 gms/ml	0.266 gms/ml	0.300 gms/ml
10.00 gms	I-5-E $\alpha_x = 42.548 \times 10^8$ L = 0.3310	I'-2-L $\alpha_x = 39.046 \times 10^8$ L = 0.3285	II-3-E $\alpha_x = 37.710 \times 10^8$ L = 0.3320	II'-8-L $\alpha_x = 38.617 \times 10^8$ L = 0.3245
16.66 gms.	III'-5-L $\alpha_x = 25.351 \times 10^8$ L = 0.5370	III-6-E $\alpha_x = 23.034 \times 10^8$ L = 0.5210	IV'-1-L $\alpha_x = 27.615 \times 10^8$ L = 0.5320	IV-2-E $\alpha_x = 28.866 \times 10^8$ L = 0.5285
23.32 gms	V'-3-L $\alpha_x = 23.073 \times 10^8$ L = 0.7240	V-7-E $\alpha_x = 19.523 \times 10^8$ L = 0.7305	VI'-7-L $\alpha_x = 22.811 \times 10^8$ L = 0.6920	VI-4-E $\alpha_x = 22.569 \times 10^8$ L = 0.7220
30.00 gms	VII-1-E $\alpha_x = 19.969 \times 10^8$ L = 0.9395	VII'-6-L $\alpha_x = 18.284 \times 10^8$ L = 0.9410	VIII-8-E $\alpha_x = 17.654 \times 10^8$ L = 0.9265	VIII'-4-L $\alpha_x = 19.525 \times 10^8$ L = 0.9290

[a]The units of α_x are ft/lb_m and the units of L are inches.

objectives of the statistical analysis were two-fold: 1) to determine whether slurry concentration and/or cake weight had a significant effect on point specific resistance, and 2) if such significant effects were apparent to determine the equation that best fit the data. From past experience on the use of the compression-permeability test cell it was thought that cake weight would probably have a larger effect than slurry concentration. Accordingly, four cake weight levels were imposed on each of the four concentrations. Since the cake weights chosen were equally spaced it was possible to make use of orthogonal polynomials in treating the data. In spacing the cake weight levels equally, it was then possible to determine the constants in the regression equation quite simply (15, 30). The advantage of using orthogonal polynomials to fit the data is that to obtain a polynomial of one higher degree all previously calculated constants can be retained and a new term calculated and added to the previous function. Orthogonal polynomial values may be obtained from the tables of Anderson and Houseman (2).

To determine the significance of the two factors in the design, the half-normal plot technique of Daniel (13) was employed. This method indicates which effects of the two factors are nonsignificant, i.e. contribute to the experimental error term, and which effects are significant. It consists of computing the single-degree-of-freedom sums of squares corre-

sponding to all the powers inherent in the two factor interactions, such as linear, quadratic, and cubic, and plotting these sums of squares on half-normal probability paper. Essentially, the empirical cumulative distribution of the single-degree-of-freedom sums of squares or contrasts is plotted. This distribution shows certain changes when there are one or more wild values in the set of observations or when the error variance is not the same for all observations. To set up this plot normal probability paper is used. For the range of P greater than 50 percent each value of P is replaced by the value $P' = 2P - 100$. The absolute value of the single-degree-of-freedom contrasts are plotted as the abscissae. The rank of the contrasts are plotted as ordinates according to the formula $P' = (i - \frac{1}{2})/n$. Thus the smallest contrast will be plotted against the lowest rank number and the largest contrast against the highest rank number. When the graph is constructed those contrasts contributing to error, i.e. those having the same error variance, will fall on the ogive, whereas those contrasts which are significant will show up as points off the curve.

With this type of graph it is possible to estimate the standard error, $\hat{\sigma}$, by noting which contrast is closest to 68.3 percent. However in estimating $\hat{\sigma}$, the contrasts which are significant should be removed and the ordinates and abscissas recalculated.

When the single-degree-of-freedom contrasts obtained from the experimental data were plotted on half normal paper the resulting graph indicated that slurry concentration had no significant effect on point specific resistance. The graph did show that cake weight had a highly significant effect. As a check on these results an analysis of variance was performed on the data. This analysis indicated the same conclusion. Figure 7 shows the half normal plot obtained from the experimental data. The significant sums of squares as obtained from the plot were terms that were constant in concentration and linear in cake weight, constant in concentration and quadratic in cake weight, constant in concentration and cubic in cake weight. From orthogonal polynomials the equation that best fit the data was

$$F(x) = 23.472 - 3.888x + 2.532x^2 - 1.327x^3 , \qquad (43)$$

where x is given by

$$x = \frac{\text{cake weight} - 20}{6.667} . \qquad (44)$$

The 95 percent confidence interval for equation 43 is

$$\text{C.I.} = F(x) \pm (t_{0.05,12})(1.935)\tfrac{1}{4}\sqrt{1 + \phi_2^2(x) + \frac{\phi_1^2(x) + \phi_3^2(x)}{5}} , \qquad (45)$$

where $\phi_1(x) = 2x$, $\phi_2(x) = x^2 - \frac{5}{4}$, and $\phi_3(x) = \frac{10}{3}(x^3 - \frac{41}{20}x)$.

The results of this experiment show how point specific resistance, as calculated from compression-permeability test

Figure 7. Half normal plot for experiment testing the effect of cake weight on point specific resistance

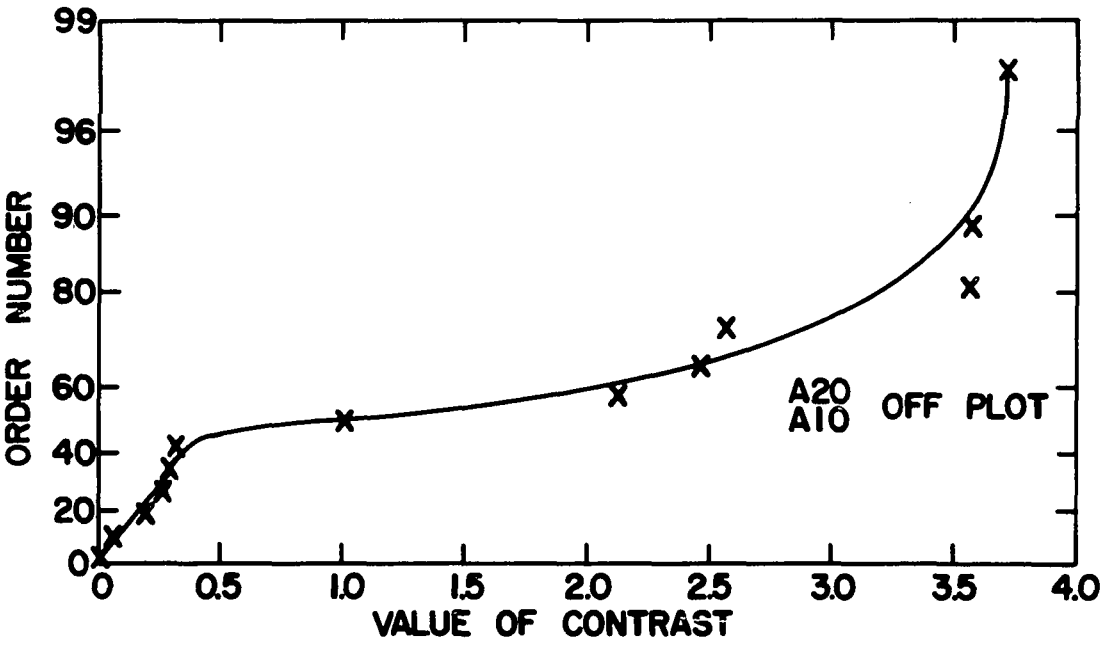
99
96
90
80
60
40
20
0
ORDER NUMBER
0
0.5
1.0
1.5
2.0
2.5
3.0
3.5
4.0
VALUE OF CONTRAST
A20
A10
OFF PLOT

cell data, varies with cake weight when the applied or solids pressure is held constant.

Part II. The Effect of Wall Friction on Compression-Permeability Testing

The only reported effect of wall friction is by Tiller.* From preliminary experimental data he indicated that up to 70 percent of the applied pressure is lost for thick cakes in a compression-permeability test cell due to friction between the cake and the cell wall. If wall friction between the cake and the cell wall does exist it may account for the variation in α_x with cake weight reported by Willis (65) and substantiated in this work. Therefore, an experiment was designed to test for wall effect.

Two compression-permeability test cells of the same material were designed and constructed. The construction of these cells was described in an earlier section. The cells differed only in diameter, one having a filtering area 3.932 times as great as the other.

The experiment was designed statistically. Four cake thicknesses were tested in each cell and the point specific resistances calculated. The cake thicknesses were designated

---

*Tiller, F. M., Dean of College of Engineering, Houston University, Houston, Texas. An hypothesis concerning wall friction. Private communication. 1962.

by the Roman numerals I, II, III, IV. The cells were designated by the Arabic numerals 1, 2; here 1 represents the small cell and 2 represents the large cell. Table 3 outlines the experiment.

Table 3. Experimental design to test for wall effect in compression-permeability test cells

Replication A				Replication B			
I	II	III	IV	I	II	III	IV
1	2	1	2	2	1	2	1
2	1	2	1	1	2	1	2
2	1	2	1	1	2	1	2
1	2	1	2	2	1	2	1

The design was balanced as far as cells and time were concerned. Four runs were made each day, thus each thickness had four units. For example, in replication A-I, cell 1 occupied the first and fourth time periods and in replication B-I, cell 1 occupied the second and third time periods. Cell 2 occupied the second and third time periods in replication A-I and the first and fourth time periods in replication B-I. This allocation was set up to eliminate any bias in the operation of the cells as far as time of day, operator, and cell were concerned. This type of grouping did not eliminate any

time trend involved, for each cell was operated in all four time periods. The grouping did insure that both cells suffered the same effect due to time if such an effect were present.

The actual conduct of the experiment was as follows. Weights of cake were chosen for cell 1. These weights were multiplied by 3.932 to give the weight of cake for cell 2. (Preliminary work indicated that this procedure gave approximately equal cake thicknesses for the two cells.) One of the two replications was chosen at random to be run first. The thicknesses in the replication were then chosen at random as to order of run. Due to the "O"-rings on the piston of each cell there was a certain amount of sliding friction between the piston and the cylinder wall. This was measured by filling the cylinder with water, adding weights to the piston, and recording the pressure by means of a 0-50 psig pressure transducer. The average pressure loss in the small cell was 1.60 psig and the average pressure loss in the large cell was 1.45 psig. Extra weight was added to the small cell to make the applied pressure the same on both cells. This applied pressure was 26.406 psig. Each run lasted one hour. The results of the experiment are summarized in Table 4.

The values of α_x in Table 4 are those at the 3600 seconds interval. At this point in the run the value of the porosity had become essentially constant. Actually the large cell was run for two hours in order to compare the value of α_x at that

Table 4. Point specific resistance, α_x, and thickness, L, for wall effect experiment[a]

Thickness I	Thickness II	Thickness III	Thickness IV
Replication A			
1 $\alpha_x = 61.4543 \times 10^8$ L = 0.4830	2 $\alpha_x = 43.7709 \times 10^8$ L = 0.6065	1 $\alpha_x = 40.6972 \times 10^8$ L = 0.6740	2 $\alpha_x = 41.2682 \times 10^8$ L = 0.8300
2 $\alpha_x = 51.4984 \times 10^8$ L = 0.4222	1 $\alpha_x = 34.5712 \times 10^8$ L = 0.5809	2 $\alpha_x = 47.0088 \times 10^8$ L = 0.7045	1 $\alpha_x = 23.7285 \times 10^8$ L = 0.7646
2 $\alpha_x = 51.6538 \times 10^8$ L = 0.4705	1 $\alpha_x = 32.5655 \times 10^8$ L = 0.5858	2 $\alpha_x = 41.4814 \times 10^8$ L = 0.6465	1 $\alpha_x = 30.2441 \times 10^8$ L = 0.7888
1 $\alpha_x = 44.1051 \times 10^8$ L = 0.4705	2 $\alpha_x = 43.7318 \times 10^8$ L = 0.5820	1 $\alpha_x = 41.0372 \times 10^8$ L = 0.6875	2 $\alpha_x = 38.5717 \times 10^8$ L = 0.8365

[a]Units of α_x are ft/lb_m and units of L are inches.

Table 4. (Continued)

Thickness			
I	II	III	IV
	Replication B		
$\alpha_x^{2} = 47.0462 \times 10^{8}$ L = 0.4410	$\alpha_x^{1} = 44.1628 \times 10^{8}$ L = 0.6200	$\alpha_x^{2} = 36.6451 \times 10^{8}$ L = 0.6700	$\alpha_x^{1} = 31.6149 \times 10^{8}$ L = 0.8865
$\alpha_x^{1} = 42.3316 \times 10^{8}$ L = 0.4638	$\alpha_x^{2} = 47.1738 \times 10^{8}$ L = 0.5640	$\alpha_x^{1} = 35.6330 \times 10^{8}$ L = 0.7362	$\alpha_x^{2} = 39.5287 \times 10^{8}$ L = 0.8302
$\alpha_x^{1} = 36.6561 \times 10^{8}$ L = 0.4825	$\alpha_x^{2} = 37.8080 \times 10^{8}$ L = 0.5119	$\alpha_x^{1} = 34.1748 \times 10^{8}$ L = 0.6930	$\alpha_x^{2} = 38.6564 \times 10^{8}$ L = 0.8110
$\alpha_x^{2} = 42.5036 \times 10^{8}$ L = 0.4268	$\alpha_x^{1} = 37.8993 \times 10^{8}$ L = 0.6080	$\alpha_x^{2} = 43.5305 \times 10^{8}$ L = 0.7497	$\alpha_x^{1} = 32.6224 \times 10^{8}$ L = 0.7609

time period with that value of α_x obtained from the small cell at 1800 seconds. This was done to obtain a comparison at the same dimension less time.

An analysis of variance was performed on the data, α_x, in Table 4. The analysis of variance used was that applicable to a split-plot design. In this design there were four thicknesses which made up the four blocks or whole plots. Each plot had two cells, in this case duplicated. It was noticed that in replication A-I the first value of cell 1, namely $\alpha_x = 61.4543 \times 10^8$, was unusually high compared to its mate, $\alpha_x = 44.1051 \times 10^8$, and the α_x values for cell 1 in replication B-I. This high value was traced to the lower pressure probe becoming clogged early in the run, thus giving an erroneous hydraulic pressure reading. This high value of α_x was dropped and replaced with its mate, which statistically is its best estimate. To account for this replacement one degree of freedom was subtracted from the measurement error term in the analysis of variance.

The data in the above design can be represented by the model

$$Y_{ijkl} = \mu + \beta_i + \gamma_j + \eta_{ij} + \rho_k + (\gamma\rho)_{jk} + \epsilon_{ijk} + \sigma_{ijkl}, \qquad (46)$$

$$i = 1, 2$$

$$j = 1, \ldots, 4$$

$$k = 1, 2$$

$$l = 1, 2$$

where β_i is the true effect of the ith replication; τ_j is the true effect of the jth thickness; η_{ij} is the whole-plot error; ρ_k is the true effect of the kth cell; $(\tau\rho)_{jk}$ is the true effect of the thickness by cell interaction for the jth thickness and kth cell; ϵ_{ijk} is the sub-plot error; and δ_{ijkl} is the measurement error associated with the ijklth combination. The δ_{ijkl} are assumed NID$(0, \sigma^2)$ in every case.

The results of the split-plot analysis of variance given in Table 5 indicated that the only significant effect was that due to cells.

The F-ratio for cells is $F_{1,4} = 23.4050$ which is highly significant. All other main effects and interactions were statistically insignificant at the 5 percent level. Previous work, as outlined in Part I, had shown that the weight of cake or thickness had a significant effect on the point specific resistance. The significance level for thickness in this analysis of variance was approximately the 15 percent level. On observing the data it is obvious that point specific resistance does decrease as thickness increases. In using the analysis of variance technique it was assumed that within each whole plot the thickness was equal. This of course was not the case since it was not experimentally possible to control thickness so precisely. However, the point specific resistance values can be adjusted for the thickness variation within each whole plot by a regression technique.

Table 5. Analysis of variance for split-plot design

Source	D.F.	S.S.	M.S.	E.M.S.
Reps (R)	1	15.2652	15.2652	$\sigma_1^2 + 2\sigma_2^2 + 4\sigma_3^2 + 16\sigma^2(\beta)$
Thick (T)	3	438.1204	146.0401	$\sigma_1^2 + 2\sigma_2^2 + 4\sigma_3^2 + 8\sigma^2(r)$
Whole-plot error	3	129.4630	43.1543	$\sigma_1^2 + 2\sigma_2^2 + 4\sigma_3^2$
Cells (C)	1	348.9984	348.9984	$\sigma_1^2 + 2\sigma_2^2 + 16\sigma^2(\rho)$
T x C	3	34.3971	11.4657	$\sigma_1^2 + 2\sigma_2^2 + 4\sigma^2(r,\rho)$
Sub-plot error	4	59.6453	14.9113	$\sigma_1^2 + 2\sigma_2^2$
Measurement error	15	157.4901	10.4993	σ_1^2
Total	30	1183.3795		

Since the combination of thickness sum of squares and cell sum of squares accounted for approximately 80 percent of the total sum of squares in the analysis of variance a regression model incorporating thickness and cell was used to represent the data. The model assumed was

$$Y_i = \beta_1 + \beta_2 T_i + \beta_3 T_i^2 + \beta_4 T_i^3 + \beta_5 z \ , \qquad (47)$$

where T_i is the observed thickness and $z = \pm 1$ depending upon whether the small cell or large cell was being used. Y_i is the observed value of α_x. A cubic model was chosen since previous work indicated that a cubic model in cake weight fit the data, and, there is a linear relationship between cake weight and cake thickness. The normal equations resulting from the regression model were solved for the β's by use of a standard multiple regression program on an IBM 7074 computer. The regression equation as calculated was

$$\hat{Y} = 78.2731 - 134.2500\ T + 168.5600\ T^2 - 82.9700\ T^3 - 3.1252\ z. \qquad (48)$$

This regression model had a multiple correlation coefficient of 0.5741. Thus the regression model used accounted for 57 percent of the total sums of squares. The remainder of the total sum of squares not accounted for by the regression model can be attributed to the various interactions and sampling error. If the quadratic and cubic terms in thickness are omitted from the model the $\hat{r}^2$ value is 0.5731. This indicates

that over the range of thickness tested little is gained by adding quadratic and cubic terms in thickness.

Equation 48 can be employed to adjust the experimental value of α_x to a common thickness value within each whole plot. The mean value of the observed thickness within each whole plot was calculated and the point specific resistance adjusted accordingly by the following equation

$$\text{adj } Y_i = Y_i\text{obs.} - \beta_2(T_i-\bar{T}) - \beta_3(T_i^2-\bar{T}^2) - \beta_4(T_i^3-\bar{T}^3) , \qquad (49)$$

or

$$\text{adj } Y_i = Y_i\text{obs.} + 134.2500(T_i-\bar{T}) - 168.5600(T_i^2-\bar{T}^2) + 82.9700(T_i^3-\bar{T}^3) . \qquad (50)$$

The new array of adjusted point specific resistance values along with the thickness for each block is shown in Table 6. The high value in replication A-I for the first value of cell 1 was again replaced by its mate.

To determine what effect the adjustment of the point specific resistance values had on the analysis of variance, the analysis was recalculated using the adjusted values. The results are shown in Table 7.

Once again the difference between cells shows as the only significant effect, although the significance level is now about 3 percent rather than 1 percent. The thickness effect still shows a significance level of approximately 15 percent. Statistically, this means that if two filter cakes of the

Table 6. Adjusted values of point specific resistance, α_x

Thickness			
I	II	III	IV
Replication A			
1 $\alpha_x = 44.6825 \times 10^8$ L = 0.4524	2 $\alpha_x = 44.3012 \times 10^8$ L = 0.5824	1 $\alpha_x = 39.7933 \times 10^8$ L = 0.6918	2 $\alpha_x = 41.6817 \times 10^8$ L = 0.8136
2 $\alpha_x = 50.4586 \times 10^8$ L = 0.4524	1 $\alpha_x = 34.5404 \times 10^8$ L = 0.5824	2 $\alpha_x = 47.2652 \times 10^8$ L = 0.6918	1 $\alpha_x = 22.6382 \times 10^8$ L = 0.8136
2 $\alpha_x = 51.3010 \times 10^8$ L = 0.4524	1 $\alpha_x = 32.6298 \times 10^8$ L = 0.5824	2 $\alpha_x = 40.5617 \times 10^8$ L = 0.6918	1 $\alpha_x = 29.6488 \times 10^8$ L = 0.8136
1 $\alpha_x = 44.6825 \times 10^8$ L = 0.4524	2 $\alpha_x = 43.7209 \times 10^8$ L = 0.5824	1 $\alpha_x = 40.9483 \times 10^8$ L = 0.6918	2 $\alpha_x = 39.1574 \times 10^8$ L = 0.8136

Table 6. (Continued)

Thickness			
I	II	III	IV
	Replication B		
$\alpha_x^2 = 46.6709 \times 10^8$ L = 0.4524	$\alpha_x^1 = 48.4054 \times 10^8$ L = 0.5824	$\alpha_x^2 = 36.2107 \times 10^8$ L = 0.6918	$\alpha_x^1 = 33.6262 \times 10^8$ L = 0.8136
$\alpha_x^1 = 42.7065 \times 10^8$ L = 0.4524	$\alpha_x^2 = 46.7502 \times 10^8$ L = 0.5824	$\alpha_x^1 = 36.5407 \times 10^8$ L = 0.6918	$\alpha_x^2 = 39.9517 \times 10^8$ L = 0.8136
$\alpha_x^1 = 37.5950 \times 10^8$ L = 0.4524	$\alpha_x^2 = 36.0876 \times 10^8$ L = 0.5824	$\alpha_x^1 = 34.2072 \times 10^8$ L = 0.6918	$\alpha_x^2 = 38.5923 \times 10^8$ L = 0.8136
$\alpha_x^2 = 41.6314 \times 10^8$ L = 0.4524	$\alpha_x^1 = 38.4518 \times 10^8$ L = 0.5824	$\alpha_x^2 = 44.7210 \times 10^8$ L = 0.6918	$\alpha_x^1 = 31.3982 \times 10^8$ L = 0.8136

Table 7. Analysis of variance using adjusted α_x values

Source	D.F.	S.S.	M.S.	E.M.S.
Reps (R)	1	6.5384	6.5384	$\sigma_1^2 + 2\sigma_2^2 + 4\sigma_3^2 + 16\sigma^2(\beta)$
Thick (T)	3	434.6316	144.8772	$\sigma_1^2 + 2\sigma_2^2 + 4\sigma_3^2 + 8\sigma^2(r)$
Whole-plot error	3	132.4355	44.1452	$\sigma_1^2 + 2\sigma_2^2 + 4\sigma_3^2$
Cells (C)	1	291.4224	291.4224	$\sigma_1^2 + 2\sigma_2^2 + 16\sigma^2(\rho)$
T x C	3	54.5220	18.1740	$\sigma_1^2 + 2\sigma_2^2 + 4\sigma^2(r,\rho)$
Sub-plot error	4	109.1831	27.2957	$\sigma_1^2 + 2\sigma_2^2$
Measurement error	15	227.7298	15.1820	σ_1^2
Total	30	1256.4628		

same thickness are tested in two compression-permeability test cells differing only in diameter different values of α_x would be expected and, in particular, higher values of α_x would be expected in the larger test cell.

Part III. Correlation of α_x with 4H/D

Experimental evidence presented and discussed above indicates that point specific resistance decreases as thickness of cake increases and that for a cake of the same thickness in two different test cells the point specific resistance is greater in the larger test cell. It has been shown that the data from a compression-permeability test cell can be represented by a cubic relationship between point specific resistance, α_x, and thickness of cake. The defining equation for α_x in terms of thickness,

$$\alpha_x = \frac{A\, g_c\, (P_2-P_1)}{\mu \rho_s (1-\epsilon_x) L \frac{dV}{d\theta}}, \qquad (51)$$

shows α_x to be inversely proportional to L and the relationship to be linear. Also, since cell geometry is not included in this equation it is apparent that the use of a particular cell should not make any significant difference in the value of α_x for a particular cake thickness.

However, if wall friction exists between the cake and the wall of the test cell, the effect should be greater in a cell

where the ratio of wall area in contact with the cake to cross-sectional area is greatest. In theory, the weight applied to the piston is transmitted by the cake to the septum. If the cake were unconfined this applied pressure would, in fact, be transmitted to the septum. However, when the cake is confined some of the applied pressure can be transmitted to the walls of the chamber by sliding friction between the cake and the walls. As a result, the cake becomes slightly less compacted and therefore should have less resistance. This situation should show up to a greater extent in the smaller diameter test cell. In this cell, for a given cake thickness, the ratio of wall area to cross-sectional area is greater than in the larger diameter cell. Because of this, more of the applied pressure would be transmitted to the wall in the small cell resulting in a cake with less resistance. This effect should also manifest itself to a greater extent with thick cakes than with thin cakes. For a given cell the ratio of wall area to cross-sectional area is greater for thick cakes; more of the applied pressure will be transmitted to the wall with a resulting decrease in compaction and, therefore, a decrease in the point specific resistance of the cake.

Considering these possibilities, it appeared desirable to investigate the relationship between α_x and H/D for the two test cells. As a first step in this direction equation 48, a

polynomial regression equation, was used to calculate values for α_x for four mean thicknesses, i.e. 0.4524 in., 0.5824 in., 0.6918 in., and 0.8136 in. for both the small and large test cells. For each thickness and each cell the ratio of wall area to cross-sectional area was calculated. This ratio simplifies to 4H/D, where H is the thickness of the cake in inches and D is the diameter of the filter chamber in inches. A plot of α_x vs. 4H/D was then made on arithmetic paper and a straight line fit to the data by the method of least squares. The graph of this least squares line is depicted in Figure 8. The least squares line fit to these predicted values of α_x is

$$\hat{Y} = 50.5935 - 8.4637\ X\ , \qquad (52)$$

where X is the ratio 4H/D and Y is the predicted value of α_x. Of significance in this least squares fit is the value of r^2, the fraction of the total sum of squares accounted for by the linear regression. In this case r^2 has a value of 0.9253 with a corresponding correlation coefficient of approximately -0.96. Thus there is a very high degree of linear correlation between α_x and 4H/D. Also of interest in this fit are the 95 percent confidence intervals for β and a. These were determined to be

$$-10.8654 \leq \beta \leq -6.0620 \qquad (53)$$

for β and

$$47.3360 \leq a \leq 53.8510 \qquad (54)$$

for a.

It is interesting that this least squares fit to the data

Figure 8. Predicted values of α_x obtained from equation 48

α_x vs. 4H/D; applied pressure = 26.406 psig
Least squares line: $\hat{Y} = 50.5935 - 8.4637\ X$

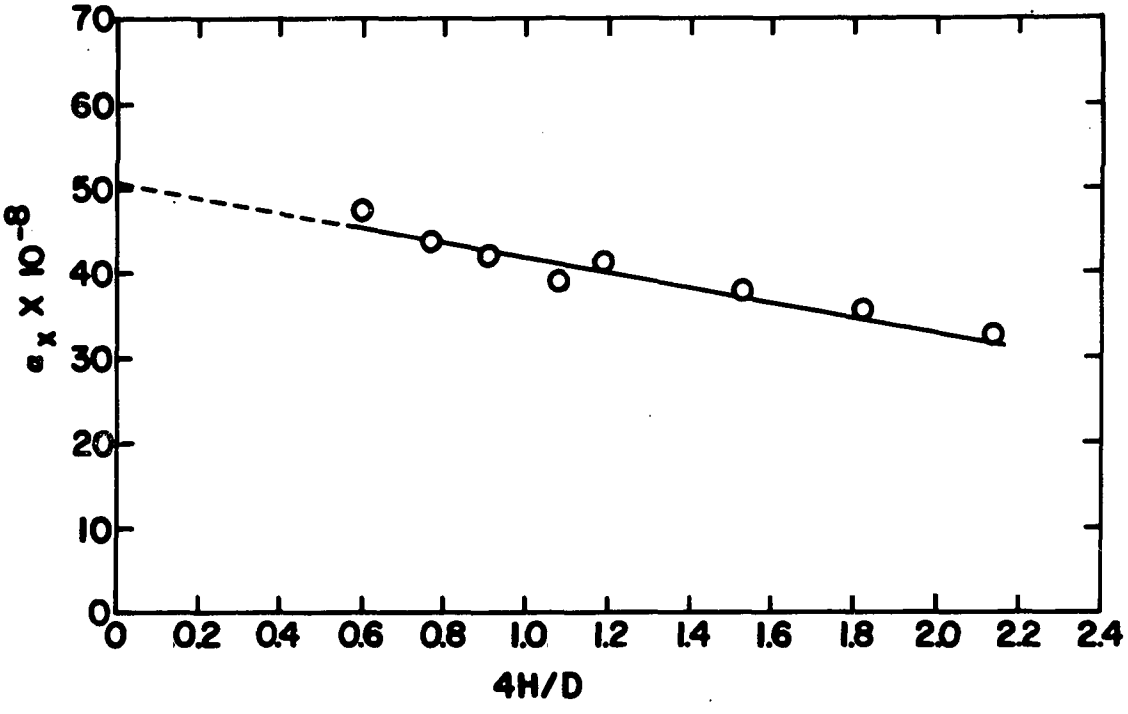
70
60
50
40
30
20
10
0
$\sigma_x \times 10^{-8}$
0
0.2
0.4
0.6
0.8
1.0
1.2
1.4
1.6
1.8
2.0
2.2
2.4
4H/D

includes values of α_x obtained from tests conducted with both the large and the small cell. Values of α_x obtained from the small cell occur at high values of 4H/D and values of α_x obtained from the large cell occur at low values of 4H/D. That a straight line fits these data with a high degree of correlation suggests that values of α_x obtained at the same 4H/D ratio from both cells should not show any significant difference. Although no data were taken to confirm this view an attempt was made to predict values of α_x by using equation 48 outside of the range for which it was obtained. There is justification for such treatment since it was shown earlier that over the range of thickness used in the experiment the data could be fit equally as well with a linear model and the quadratic and cubic terms do not contribute much to the value of α_x.

Values of α_x were estimated for the small cell for thickness chosen to give the same 4H/D ratio that occurred in the large cell. An estimate of the variance of these four values of α_x for the small cell was calculated along with an estimate of the variance of the four values of α_x previously estimated for the large cell. An F-test indicated no significant difference between the variances of the α_x values obtained from the two cells.

The actual experimental values of α_x which had been adjusted for thickness variations were then plotted against

4H/D. In this case the mean value of α_x for each cell in each thickness level was calculated and plotted. A least squares line was fit to the data. The equation of this line was found to be

$$\hat{Y} = 51.5190 - 9.1135\ X\ , \qquad (55)$$

where X is 4H/D and $\hat{Y}$ is the estimated value of α_x. This graph is shown in Figure 9. It is obvious that both the estimate of β, -9.1135, and a, 51.5190, fall within the confidence intervals calculated above. The value of r^2 for this fit is 0.8496 giving a correlation coefficient r of approximately -0.92.

Both equations 52 and 55 were fit to data obtained at an applied pressure of 26.406 psig. It would be expected that the straight line describing these data would move up or down depending upon whether the applied pressure was increased or decreased.

The steel cell used in Part I had a pressure loss of 3.90 psig, as measured by Willis (64); with the weights added to the piston in this experiment the applied pressure, taking into account the 3.90 psig pressure loss, was 23.123 psig. Therefore considering the foregoing discussion it would be expected that the value of the intercept, a, calculated from a least squares line fit to the data would be less than the values reported above. The 16 values of α_x obtained from the steel cell were plotted against their respective 4H/D values

Figure 9. Experimental values of α_X adjusted by equation 48

α_X vs. 4H/D; applied pressure = 26.406 psig
Least squares line: $\hat{Y} = 51.5190 - 9.1135\ X$

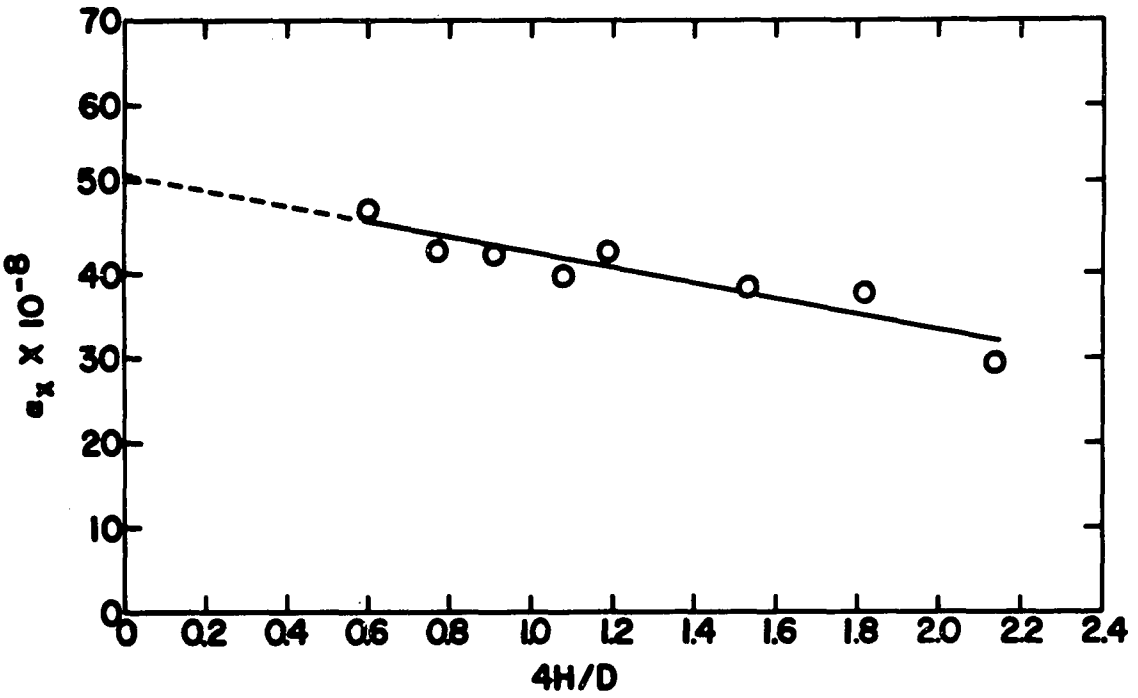
70
60
50
40
30
20
10
0
$\epsilon_x \times 10^{-8}$
0
0.2
0.4
0.6
0.8
1.0
1.2
1.4
1.6
1.8
2.0
2.2
2.4
4H/D

Figure 10. Values of α_x obtained from steel cell used in Part I

α_x vs. 4H/D; applied pressure = 23.123 psig
Least squares line: $\hat{Y} = 47.213 - 13.325\ X$

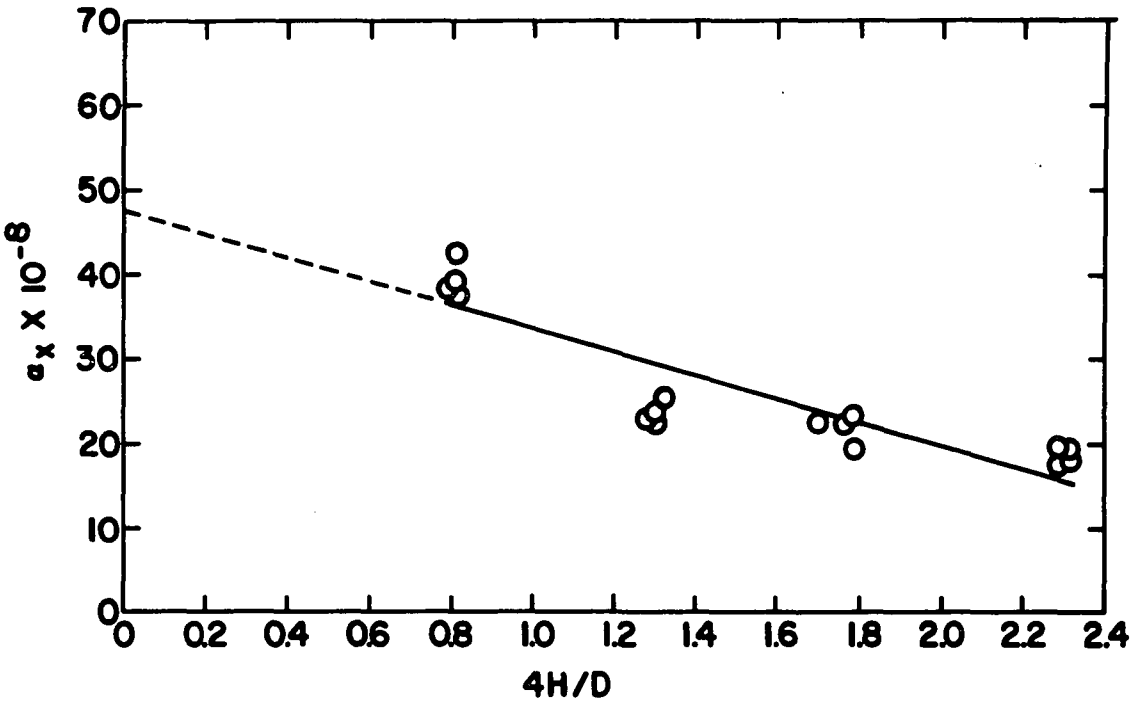
70
60
50
40
30
20
10
0
$a_x \times 10^{-8}$
0
0.2
0.4
0.6
0.8
1.0
1.2
1.4
1.6
1.8
2.0
2.2
2.4
4H/D

and a least squares line fit to the data. The equation of this line, the graph of which is shown in Figure 10, was

$$\hat{Y} = 47.213 - 13.325\ X. \qquad (56)$$

As expected, the value of a, 47.213, was less than that calculated at the higher applied pressure. The value of r^2 for this least squares fit was 0.8376, giving a value of r = -0.915.

From these investigations, it is apparent that wall effect must be taken into account when interpreting compression-permeability test cell data. This effect has not been accounted for in previous work and may, therefore, account for some of the spurious results obtained. In order to predict filtration resistances from test cell data it has been the custom to measure the specific resistance of a cake in a test over the range of pressure under which the actual filtration would proceed. However, it is assumed when using the test cell that the point specific resistance of a differential element of filter cake is measured, whereas in reality the specific resistance of a finite cake is measured. The correlation of α_x with 4H/D makes it possible to obtain the point specific resistance of the differential element of filter cake. By measuring the specific resistances of two or three cakes of different thickness in a test cell and plotting the values of α_x so obtained against the 4H/D ratio corresponding to the particular thickness, the straight line through these

points extrapolated to zero 4H/D would essentially give the point specific resistance of a differential element of filter cake at that applied pressure. Following this procedure it is quite likely that a better correlation between test cell data and constant pressure filtration data would result.

CONCLUSIONS

The results of this investigation have shown that if two filter cakes having the same thickness are tested in two test cells, differing only in diameter, the point specific resistance of the two cakes differ. A statistical analysis of the data indicates that this difference is significant. The filter cake tested in the cell with the greater diameter possesses a larger point specific resistance. Since the equation used to calculate the point specific resistance indicates that cakes of the same thickness under the same applied pressure should possess equal point specific resistances, this difference is attributed to a wall effect between the filter cake and the wall of the test cell.

It has been shown that the wall effect can be removed if α_x is plotted against the ratio of wall area in contact with the cake to the cross-sectional area of the septum. This ratio is 4H/D, where H is cake thickness and D is cell diameter. A straight line results. The intercept of this line at zero 4H/D is the point specific resistance of a differential element of filter cake at the particular applied pressure.

RECOMMENDATIONS

Further work needs to be done on the correlation of the results from compression-permeability tests with constant pressure filtration results. In particular, it is recommended that:

1. Experiments be conducted using the 4H/D zero intercept values of α_x as the point specific resistance values of a differential element of filter cake. When these values, obtained over the range of pressure used in a constant pressure filtration, are averaged and compared with the average specific resistance obtained from the constant pressure filtration a high degree of correlation should be indicated.
2. The test cells should be modified to obtain more accurate hydraulic pressure readings. This could be done by using pressure transducers.

REFERENCES

1. Almy, C., Jr. and Lewis, W. K. Factors determining the capacity of a filter press. J. Ind. Engr. Chem. 4: 528-532. 1912.

2. Anderson, R. L. and Houseman, E. E. Tables of orthogonal polynomial values extended to N = 104. Iowa Agr. Expt. Sta. Bul. 297. 1942.

3. Badger, W. L. and Banchero, J. T. Introduction to chemical engineering. N.Y., McGraw-Hill Book Co., Inc. 1955.

4. Baker, F. P. A study of the fundamental laws of filtration using plant-scale equipment. J. Ind. Engr. Chem. 13: 610-612. 1921.

5. Bakker, P. J., Heertjes, P. M., and Hibou, J. L. The influence of the initial filtration velocity and of vibrations on the resistance of a polystyrene filter-cake. Chem. Engr. Sci. 10: 139-149. 1959.

6. Bonilla, C. F. Interpretation of constant rate filtration data. Am. Inst. Chem. Engrs. Trans. 34: 243-250. 1938.

7. Brenner, H. Three-dimensional filtration on a circular leaf. Am. Inst. Chem. Engrs. J. 7: 666-671. 1961.

8. Burak, N. and Storrow, J. A. Hydroextraction. I. The flow relationships in a basket centrifuge. Soc. Chem. Ind. (London) J. 69: 8-13. 1950.

9. Carman, P. C. Fluid flow through granular beds. Inst. Chem. Engrs. (London) Trans. 15: 150-166. 1937.

10. Carman, P. C. Fundamental principles of industrial filtration. Inst. Chem. Engrs. (London) Trans. 16: 168-188. 1938.

11. Carman, P. C. A study of the mechanism of filtration. I. Soc. Chem. Ind. (London) J. 52: 280T-282T. 1933.

12. Carman, P. C. A study of the mechanism of filtration. II. Soc. Chem. Ind. (London) J. 53: 301T-309T. 1934.

13. Daniel, C. Use of half-normal plots in interpreting factorial two-level experiments. Technometrics 1: 311-341. 1959.

14. Darcy, H. P. G. Les fontaines publiques de la ville de Dijon. Paris, Victor Dalmont. 1856. Original not available; cited by Hubbert, M. K. Darcy's law and the field equations for the flow of underground fluids. Bul. de l'Assoc. Intl. d'Hydrol. Sci. 5: 25. 1957.

15. Davies, O. L., ed. Statistical methods in research and production. London, Oliver and Boyd. 1957.

16. Dupuit, A. J. Etudes theoretiques et practiques sur le mouvement des eaux. 1863. Original not available; cited by Carman, P. C. Fundamental principles of industrial filtration. Inst. Chem. Engrs. (London) Trans. 16: 171. 1938.

17. Fair, G. H. and Hatch, L. P. Fundamental factors governing the streamline flow of water through sand. Am. Water Works Assoc. J. 25: 1551-1565. 1933.

18. Foust, A. S., Wenzel, L. A., Clump, C. W., Maus, L., and Anderson, L. B. Principles of unit operations. N. Y., John Wiley and Sons, Inc. 1960.

19. Grace, H. P. Resistance and compressibility of filter-cakes. Chem. Engr. Prog. 49: 303-318. 1953.

20. Grace, H. P. Resistance and compressibility of filter-cakes. II. Under conditions of pressure filtration. Chem. Engr. Prog. 49: 367-377. 1953.

21. Grace, H. P. Resistance and compressibility of filter-cakes. III. Under conditions of centrifugal filtration. Chem. Engr. Prog. 49: 427-436. 1953.

22. Haruni, M. M. and Storrow, J. A. Hydroextraction. VIII. Cake formation. Chem. Engr. Sci. 3: 43-47. 1954.

23. Haruni, M. M., Todhunter, K. H., and Storrow, J. A. Hydroextraction. IX. Studies of flow through incompressible cakes. Chem. Engr. Sci. 3: 87-96. 1954.

24. Hatscheck, E. The mechanism of filtration. Soc. Chem. Ind. (London) J. 27: 538-544. 1908.

25. Heertjes, P. M. Industrial filtrations. Research 3: 254-259. June, 1950.

26. Hinchley, J. W., Ure, S. G. M., and Clarke, B. W. Studies in filtration. Soc. Chem. Ind. (London) J. 45: 1T-10T. 1926.

27. Hubbert, M. K. Darcy's law and the field equations of the flow of underground fluids. Bul. de l'Assoc. Intl. d'Hydrol. Sci. 5: 24-59. 1957.

28. Hutto, F. B., Jr. Distribution of porosity in filter-cakes. Chem. Engr. Prog. 53: 328-332. 1957.

29. Igmanson, W. L., Andrews, B. D., and Johnson, R. C. Internal pressure distributions in compressible mats under fluid stress. Tech. Assoc. Pulp and Paper Ind. J. 42: 840-849. 1959.

30. Kendall, M. G. The advanced theory of statistics. Vol. II. London, Charles Griffin and Company, Limited. 1946.

31. Kottwitz, F. A. Prediction of filtration resistance by compression-permeability techniques. Unpublished Ph.D. thesis. Ames, Iowa, Library, Iowa State University of Science and Technology. 1955.

32. Kozeny, J. Kapillare Leitung des Wassers im Boden. Osterreichische Akademie der Wissenschaften. Mathematisch naturwissen schaftliche klasse, Sitzungsberichte Abt. IIa, 136: 271-306. 1927.

33. Kruger, E. Die Grundwasserbewegung. Internationale Mitteilungen für Bodenkunde. 8: 105-122. 1918.

34. Miller, S. A. Recent advances in filtration theory. Chem. Engr. Prog. 47: 497-502. 1951.

35. Okamura, S. and Shirato, M. Liquid pressure distribution within cakes in constant pressure filtration. Chemical Engineering (Japan) 19: 104-100. 1955.

36. Okamura, S. and Shirato, M. p_x-distribution within cakes in compression-permeability testing. Chemical Engineering (Japan) 19: 111-119. 1955.

37. Okamura, S. and Shirato, M. The aging of ignition-plug slurries and the accuracy of the prediction of filtration. Chemical Engineering (Japan) 20: 98-105. 1956.

38. Ostle, B. Statistics in research. Ames, Iowa, Iowa State University Press. 1954.

39. Ruth, B. F. Correlating filtration theory with industrial practice. J. Ind. Engr. Chem. 38: 564-571. 1946.

40. Ruth, B. F. Studies in filtration. III. Determination of general filtration equation. J. Ind. Engr. Chem. 27: 708-723. 1935.

41. Ruth, B. F., Montillon, G. A., and Montanna, R. E. Comments upon recent developments in the theory of filtration. J. Ind. Engr. Chem. 23: 850-851. 1931.

42. Ruth, B. F., Montillon, G. A., and Montanna, R. E. Studies in filtration. I. Critical analysis of filtration theory. J. Ind. Engr. Chem. 25: 76-82. 1933.

43. Ruth, B. F., Montillon, G. A., and Montanna, R. E. Studies in filtration. II. Fundamental axiom of constant-pressure filtration. J. Ind. Engr. Chem. 25: 153-161. 1933.

44. Scheidegger, A. E. The physics of flow through porous media. Toronto, University of Toronto Press. 1960.

45. Seelheim, F. Methoden sur Bestimmung der Durchlassigkeit des Bodens. Zeitschrift für analytische Chemie. 19: 387-418. 1880.

46. Shirato, M. and Okamura, S. Behavior of gairome-clay slurries at constant-pressure filtration. Chemical Engineering (Japan) 20: 678-684. 1956.

47. Sperry, D. R. Analysis of filtration data. J. Ind. Engr. Chem. 36: 323-329. 1944.

48. Sperry, D. R. Effect of pressure on fundamental filtration when solids are non-rigid or deformable. J. Ind. Engr. Chem. 20: 892-895. 1928.

49. Sperry, D. R. A new method of conducting filtration tests. J. Ind. Engr. Chem. 18: 276-278. 1926.

50. Sperry, D. R. A study of the fundamental law of filtration using plant-scale equipment. I. J. Ind. Engr. Chem. 13: 1163-1165. 1921.

51. Tiller, F. M. The role of porosity in filtration. I. Chem. Engr. Prog. 49: 467-479. 1953.

52. Tiller, F. M. The role of porosity in filtration. II. Chem. Engr. Prog. 51: 282-290. 1955.

53. Tiller, F. M. The role of porosity in filtration. III. Am. Inst. Chem. Engrs. J. 4: 170-174. 1958.

54. Tiller, F. M. and Cooper, H. R. The role of porosity in filtration. IV. Am. Inst. Chem. Engrs. J. 6: 585-601. 1960.

55. Tiller, F. M. and Cooper, H. R. The role of porosity in filtration. V. Am. Inst. Chem. Engrs. J. 8: 445-449. 1962.

56. Tiller, F. M. and Shirato, M. The role of porosity in filtration. VI. Am. Inst. Chem. Engrs. J. 10: 61-67. 1964.

57. Van Gilse, J. P. M., Van Ginneken, P. J. H., and Waterman, H. I. Studies in filtration. I. J. Soc. Chem. Ind. (London) 49: 444T-446T. 1930.

58. Van Gilse, J. P. M., Van Ginneken, P. J. H., and Waterman, H. I. Studies in filtration. II. J. Soc. Chem. Ind. (London) 49: 483T-490T. 1930.

59. Van Gilse, J. P. M., Van Ginneken, P. J. H., and Waterman, H. I. Studies in filtration. III. J. Soc. Chem. Ind. (London) 50: 41T-44T. 1931.

60. Van Gilse, J. P. M., Van Ginneken, P. J. H., and Waterman, H. I. Studies in filtration. IV. J. Soc. Chem. Ind. (London) 50: 95T-100T. 1931.

61. Walas, S. M. Resistance to filtration. Trans. Am. Inst. Chem. Engrs. 42: 783-793. 1946.

62. Walker, W. H., Lewis, W. K., and McAdams, W. H. Principles of chemical engineering. N. Y., McGraw-Hill Book Co., Inc. 1927.

63. Webber, H. C. and Hershey, R. L. Some practical applications of the Lewis equation. J. Ind. Engr. Chem. 18: 341-344. 1926.

64. Willis, M. S. Compression-permeability testing with calcium carbonate. Unpublished M.S. thesis. Ames, Iowa, Library, Iowa State University of Science and Technology. 1959.

65. Willis, M. S. Correlation of compression-permeability testing with filtration. Unpublished Ph.D. thesis. Ames, Iowa, Library, Iowa State University of Science and Technology. 1962.

ACKNOWLEDGEMENTS

The author would like to express his appreciation to Dr. D. R. Boylan for suggesting the problem and for his guidance throughout the course of the work.

The author also expresses his appreciation to Dr. H. T. David, Professor of Statistics, for his unfailing good humor and the many hours he spent discussing the statistical portion of the work.

Appreciation is also extended to Mr. W. D. Lawing, graduate student in statistics, for helpful discussions on the statistical analysis.

Last but not least, the author is indebted to the Iowa Engineering Experiment Station for financial support during the course of the work.

APPENDIX A: LEAST SQUARES LINE FOR α_x vs. 4H/D; VALUES OF α_x PREDICTED FROM EXPERIMENTAL REGRESSION EQUATION APPLIED PRESSURE = 26.406 PSIG

$Y = \alpha_x$, $X = 4H/D$

Y	X	Y	X
47.4848	0.6012	41.2344	1.1921
43.9918	0.7740	37.7414	1.5346
41.7255	0.9193	35.4751	1.8229
39.0631	1.0812	32.8127	2.1438

Least squares line: $\hat{Y} = \hat{a} + bX$

$\sum X = 10.0691$ $\quad \sum Y = 319.5288$ $\quad \sum XY = 385.2757$

$\bar{X} = 1.2586$ $\quad \bar{Y} = 39.9411$ $\quad \frac{\sum X \sum Y}{n} = 402.1709$

$(\sum X)^2 = 101.3868$ $\quad (\sum Y)^2 = 102098.6540$

$(\sum X)^2/n = 12.6734$ $\quad (\sum Y)^2/n = 12762.3317$

$\sum X^2 = 14.6696$ $\quad \sum Y^2 = 12916.8728$

$\sum x^2 = 1.9962$ $\quad \sum y^2 = 154.5411$

$$b = \frac{\sum XY - \frac{\sum X \sum Y}{n}}{\sum x^2} = -8.4637$$

$\hat{a} = \bar{Y} - b\bar{X} = 50.5935$

$\hat{Y} = 50.5935 - 8.4637\ X$

$$r^2 = \frac{(\sum xy)^2}{\sum x^2 \sum y^2} = \frac{(-16.8952)^2}{(1.9962)(154.5411)} = 0.9253$$

95% Confidence Interval for β

$$S.S.E. = \frac{\sum y^2 - \frac{(\sum xy)^2}{\sum x^2}}{n-2} = \frac{154.511 \quad \frac{285.4478}{1.9962}}{6} = 1.9242$$

$$s_b^2 = \frac{S.S.E.}{x^2} = \frac{1.9242}{1.9962} = 0.9639 \; ; \quad s_b = \sqrt{s_b^2} = 0.9815$$

$$t_{6,0.05} = 2.447$$

$$s_b t = 2.4017$$

$$b - s_b t \leq \beta \leq b + s_b t$$

$$-10.8654 \leq \beta \leq -6.0620$$

95% Confidence Interval for a

$$L_1 = \hat{a} - t_{6,0.05}\, s_E \sqrt{\frac{1}{n} + \frac{\bar{X}^2}{\sum x_i^2}}$$

$$L_2 = \hat{a} + t_{6,0.05}\, s_E \sqrt{\frac{1}{n} + \frac{\bar{X}^2}{\sum x_i^2}}$$

$$L_1 = 50.5935 - 3.2575 = 47.3360$$

$$L_2 = 50.5935 + 3.2575 = 53.8510$$

$$L_1 \leq a \leq L_2$$

$$47.3360 \leq a \leq 53.8510$$

APPENDIX B: LEAST SQUARES LINE FOR EXPERIMENTAL VALUES OF α_x ADJUSTED BY EXPERIMENTAL REGRESSION EQUATION; α_x vs. 4H/D; APPLIED PRESSURE = 26.406 PSIG

Y	X	Y	X
42.4166	1.1921	47.5155	0.6012
38.5068	1.5346	42.7150	0.7740
37.8724	1.8229	42.1896	0.9193
29.3278	2.1438	39.8458	1.0812

Least squares line: $\hat{Y} = \hat{a} + bX$

$\sum X = 10.0691$ $\quad \sum Y = 320.3895$ $\quad \sum XY = 385.0618$

$\bar{X} = 1.2586$ $\quad \bar{Y} = 40.0487$ $\quad \frac{\sum X \sum Y}{n} = 403.2542$

$(\sum X)^2 = 101.3868$ $\quad (\sum Y)^2 = 102649.4317$

$(\sum X)^2/n = 12.6734$ $\quad (\sum Y)^2/n = 12831.1790$

$\sum x^2 = 14.6696$ $\quad \sum y^2 = 13026.3242$

$\sum x^2 = 1.9962$ $\quad \sum y^2 = 195.1452$

$$b = \frac{\sum XY - \frac{\sum X \sum Y}{n}}{\sum x^2} \qquad \frac{385.0618 - 403.2542}{1.9962} = -9.1135$$

$$\hat{a} = \bar{Y} - b\bar{X} = 40.0487 + 9.1135(1.2586) = 51.5190$$

$$\hat{Y} = 51.5190 - 9.1135\,X$$

$$r^2 = \frac{(\sum xy)^2}{\sum x^2 \sum y^2} \qquad \frac{330.9634}{(1.9962)(195.1542)} = 0.8496$$

APPENDIX C: LEAST SQUARES LINE FOR VALUES OF α_x OBTAINED FROM STEEL CELL; α_x vs. 4H/D; APPLIED PRESSURE = 23.123 PSIG

Y	X	Y	X
42.548	0.8148	37.710	0.8127
25.351	1.3218	27.615	1.3095
23.073	1.7821	22.811	1.7033
19.969	2.3126	17.654	2.2806
39.046	0.8086	38.617	0.7988
23.034	1.2824	28.866	1.3009
19.523	1.7981	22.569	1.7772
18.284	2.3163	19.525	2.2867

Least squares line: $\hat{Y} = \hat{a} + bX$

$\sum X = 24.7064$ $\quad \sum Y = 426.195$ $\quad \sum XY = 593.124$

$\bar{X} = 1.5442$ $\quad \bar{Y} = 26.637$ $\quad \frac{\sum X \sum Y}{n} = \frac{10529.744}{16} = 658.109$

$(\sum X)^2 = 610.4062$ $\quad (\sum Y)^2 = 181642.178$

$(\sum X)^2/n = 38.1504$ $\quad (\sum Y)^2/n = 11352.636$

$\sum X^2 = 43.0273$ $\quad \sum Y^2 = 12386.479$

$\sum x^2 = 4.8769$ $\quad \sum y^2 = 1033.843$

$$b = \frac{593.124 - 658.109}{4.8769} = -13.325$$

$\hat{a} = \bar{Y} - b\bar{X}$

$\hat{a} = 26.637 + 13.325(1.5442)$

$\hat{a} = 47.213$

$\hat{Y} = 47.213 - 13.325\ X$

95% Confidence Interval for β

$$S.S.E. = \frac{1033.843 - 865.911}{14} = 11.995 \qquad s_b^2 = \frac{11.995}{4.877} = 2.460$$

$$r^2 = \frac{4223.050}{(4.8769)(1033.843)} = 0.8376 \qquad s_b = 1.57$$

$$t_{14,0.05} = 2.145$$

$$L_1 = b - s_b t_{14,0.05} = -13.325 - 1.57(2.145) = -16.693$$

$$L_2 = b + s_b t_{14,0.05} = -13.325 + 3.368 = -9.957$$

$$-16.693 \leq \beta \leq -9.957$$

95% Confidence Interval for a

$$L_1 = \hat{a} - t_{0.05,(14)}\, s_E \sqrt{\frac{1}{n} + \frac{\bar{X}^2}{\sum x^2}}$$

$$L_2 = \hat{a} + t_{0.05,(14)}\, s_E \sqrt{\frac{1}{n} + \frac{\bar{X}^2}{\sum x^2}}$$

$$L_1 = 47.213 - 5.519 = 41.694$$

$$L_2 = 47.213 + 5.519 = 52.732$$

$$L_1 \leq a \leq L_2$$

$$41.694 \leq a \leq 52.732$$

APPENDIX D: FORTRAN PROGRAM FOR THE CALCULATION OF α_x

```
C     SPECIFIC RESISTANCE CALCULATION
  100 WRITE OUTPUT TAPE 2,1
    1 FORMAT (10X,3HPOR,14X,1HQ,15X,4HDELP,12x,5HALPHA)
   12 FORMAT (I5)
      READ INPUT TAPE 1,12, NUMB
      DO 14 I=1,NUMB
    2 READ INPUT TAPE 1,3,W,H,A,V,T,PRES,RHO,ZMU
    3 FORMAT (F8.4,1X,F6.4,1X,F8.6,1X,F5.2,1X,F5.2,1X,F5
     1.2,1X,F7.4,1X,F10.8)
    4 POR=1.0-(W*12.0)/(182.83*H*A*453.59)
      Q=V/(T*A*28320.0)
      DELP=(PRES*RHO)/30.48
      ALPHA=(32.2*A*DELP)/(Q*ZMU*(W/453.59))
      WRITE OUTPUT TAPE 2,10,POR,Q,DELP,ALPHA
   10 FORMAT (5X,F12.6,4X,F12.8,5X,F12.4,4X,F13.1)
   14 CONTINUE
    5 STOP
      END
```

APPENDIX E: DATA FOR COMPRESSION-PERMEABILITY TESTS DESCRIBED IN PART I

Table 8. Data for compression-permeability tests described in Part I (Test material - reagent grade $CaCO_3$; applied pressure - 23.123 psig)

Run no.	Cake weight (gms.)	Por.	Thick. (in.)	$Qx10^3$ ft^3/ft^2sec	P lb_t/ft^2	$\alpha_x x10^{-8}$ ft/lb_m	T °C
VII-E-1	30.00	0.6770	0.9395	0.6754	110.3727	19.9687	27.0
IV-E-2	16.66	0.6833	0.5285	0.7877	108.1861	28.8662	25.0
II-E-3	10.00	0.6974	0.3320	0.9122	93.8474	37.7103	25.0
VI-E-4	23.32	0.6755	0.7220	0.7184	107.9819	22.5690	25.0
I-E-5	10.00	0.6964	0.3310	0.9926	112.7824	42.5483	25.0
III-E-6	16.66	0.6787	0.5210	0.9182	100.6335	23.0337	25.0
V-E-7	23.32	0.6793	0.7305	0.7661	99.6128	19.5230	25.0
VIII-E-8	30.00	0.6747	0.9265	0.6626	100.2252	17.6544	25.0
IV'-L-1	16.66	0.6854	0.5320	0.7752	104.1288	27.6148	24.0
I'-L-2	10.00	0.6941	0.3285	0.9097	96.9076	39.0456	27.0
VI-L-3	23.32	0.6764	0.7240	0.7096	111.4791	23.0726	24.0
VIII'-L-4	30.00	0.6755	0.9290	0.6494	111.0708	19.5246	24.0
III'-L-5	16.66	0.6883	0.5370	0.7497	90.4272	25.3510	25.0
VII'-L-6	30.00	0.6797	0.9410	0.6072	95.1221	18.2841	25.0
VI'-L-7	23.32	0.6614	0.6920	0.6906	104.9201	22.8113	25.0
II'-L-8	10.00	0.6903	0.3245	0.1066	109.9272	38.6169	28.0

APPENDIX F: DATA FOR COMPRESSION-PERMEABILITY TESTS DESCRIBED IN PART II

Table 9. Data for compression-permeability tests described in Part II (Material tested - reagent grade $CaCO_3$; applied pressure - 26.406 psig)

Run no.	Cake weight (gms.)	Por.	Thick. (in.)	$Qx10^3$ ft^3/ft^2sec	P lb_t/ft^2	$\alpha_x x10^{-8}$ ft/lb_m	T °C
I-1-A-1	14.9990	0.6424	0.4830	0.3849	124.9028	61.4543	22.0
I-1-A-2	15.0106	0.6327	0.4705	0.5281	121.2122	44.1051	22.5
I-1-B-1	58.9555	0.5911	0.4222	0.4795	125.3740	51.4984	23.5
I-1-B-2	58.9857	0.6091	0.4705	0.4701	124.7739	51.6538	23.0
I-2-A-1	18.9992	0.6234	0.5809	0.4568	113.1337	34.5712	19.0
I-2-A-2	18.9990	0.6266	0.5858	0.5108	119.1634	32.5655	19.0
I-2-B-1	74.6986	0.6394	0.6065	0.3664	112.0891	43.7709	20.0
I-2-B-2	74.7098	0.6242	0.5820	0.3841	114.6207	43.7318	21.0
I-3-A-1	23.0013	0.5907	0.6740	0.3566	124.2608	40.6972	19.5
I-3-A-2	22.9993	0.6148	0.6875	0.3707	125.3221	41.0373	22.0
I-3-B-1	90.4439	0.6241	0.7045	0.3176	123.3041	47.0088	21.0
I-3-B-2	90.4339	0.5904	0.6465	0.3721	127.4925	41.4814	21.0
I-4-A-1	26.9974	0.5934	0.7646	0.4460	109.2611	23.7785	18.5
I-4-A-2	26.9973	0.6059	0.7888	0.3673	115.9162	30.2441	18.0
I-4-B-1	106.1624	0.6255	0.8300	0.2946	117.8897	41.2682	21.0
I-4-B-2	106.1647	0.6284	0.8365	0.2928	112.1912	38.5117	20.0
II-1-A-1	14.9981	0.6277	0.4638	0.4225	106.3289	42.3316	17.0
II-1-A-2	14.9988	0.6421	0.4825	0.4746	106.1352	36.6561	16.0
II-1-B-1	58.9795	0.6084	0.4410	0.4046	108.9544	47.0462	18.5
II-1-B-2	58.9789	0.5954	0.4268	0.4701	110.2499	42.5036	20.0

Table 9. (Continued)

Run no.	Cake weight (gms.)	Por.	Thick. (in.)	$Qx10^3$ ft^3/ft^2sec	P lb_t/ft^2	$\alpha_x x10^{-8}$ ft/lb_m	T °C
II-2-A-1	19.0007	0.6471	0.6200	0.3658	116.4041	44.1628	19.0
II-2-A-2	18.9989	0.6402	0.6080	0.4446	112.2485	37.8993	22.0
II-2-B-1	74.7076	0.6122	0.5640	0.3627	113.9849	47.1738	22.0
II-2-B-2	74.7177	0.5823	0.5119	0.4154	107.1632	37.8080	21.0
II-3-A-1	22.9974	0.6403	0.7362	0.3957	111.0917	35.6330	23.0
II-3-A-2	22.9980	0.6179	0.6930	0.4270	114.9717	34.1748	23.0
II-3-B-1	90.4400	0.6048	0.6700	0.3753	107.0988	36.6451	23.5
II-3-B-2	90.4352	0.6468	0.7497	0.3419	114.5403	43.5305	24.0
II-4-A-1	26.9991	0.6493	0.8865	0.3129	107.2491	31.6149	16.5
II-4-A-2	26.9978	0.5915	0.7609	0.3469	112.3956	32.6224	20.0
II-4-B-1	106.1652	0.6256	0.8302	0.2748	107.8998	39.5287	20.0
II-4-B-2	106.1645	0.6167	0.8110	0.2858	109.7390	38.6564	20.0